

Variants of SGD for Lipschitz Continuous Loss Functions in Low-Precision Environments

Michael R. Metel*

Huawei Noah's Ark Lab, Montréal, Qc, Canada

December 26, 2022

Abstract

Motivated by neural network training in low-bit floating and fixed-point environments, this work studies the convergence of variants of SGD with computational error. Considering a general stochastic Lipschitz continuous loss function, a novel convergence result to a Clarke stationary point is presented assuming that only an approximation of its stochastic gradient can be computed as well as error in computing the SGD step itself. Different variants of SGD are then tested empirically in a variety of low-precision arithmetic environments, where improved test set accuracy is observed compared to SGD for two image recognition tasks.

1 Introduction

This paper studies the convergence of variants of stochastic gradient descent (SGD) in an environment with non-negligible computational error. The assumptions are given in a general form but are motivated by the error from using low-bit finite precision arithmetic for neural network training. Given the continuously increasing size of deep learning models, there is a strong motivation to do training in lower-bit environments. The majority of research in this area is focused on hardware design using number formats of different precision for different types of data (gradients, weights, etc.) to accelerate training and reduce memory requirements while aiming to incur minimal accuracy degradation, see (Wang et al., 2022, Table 1). Our work is complementary to this line of research, with a focus on trying to gain a better understanding of low-bit training from the perspective of the training algorithm, namely, we seek to understand what level of error can be imposed while still maintaining a theoretical convergence guarantee, and to observe empirically to what extent simple variants of SGD can improve a model's accuracy in challenging low-bit environments.

The theoretical convergence analysis in Section 5 focuses on using perturbed SGD (PSGD)

*michael.metel@huawei.com

to find a stationary point to the problem

$$\min_{w \in \mathbb{R}^d} f(w) := \mathbb{E}[F(w, \xi)], \quad (1)$$

where $\xi \in \mathbb{R}^r$ is a random vector from a probability space (Ω, \mathcal{F}, P) , and $F(w, \xi)$ is assumed to be a stochastic Lipschitz continuous function in $w \in \mathbb{R}^d$, with the precise details given in Section 2. Unlike assuming that $F(w, \xi)$ is convex or that it has a Lipschitz continuous gradient, this assumption is much closer to reality as a wide range of neural network architectures are known to be at least locally Lipschitz continuous (Davis et al., 2020).

Section 6 examines the empirical performance of variants of SGD, focusing on image recognition tasks in floating and fixed-point environments. Given that the training was performed in low-bit settings with observed variation in accuracy over different runs, emphasis was placed on algorithms' robustness, with their evaluation based not only on their average, but also their worst-case accuracy.

Before these results, an overview of floating and fixed-point arithmetic using rounding to nearest and stochastic rounding is given in Section 3. In Section 4, relevant past work studying optimization with computational error is discussed, with the paper concluding in Section 7. Sections numbered greater than 7 are in the Appendix, which contains all of the proofs of the theoretical results, as well as the detailed results and plots from the numerical experiments.

2 Lipschitz Continuous Loss Functions

This section contains the required assumptions and resulting properties for functions $f(w)$ of form (1). It is assumed that $F(w, \xi)$ is continuous in w for each $\xi \in \mathbb{R}^r$, and Borel measurable in ξ for each $w \in \mathbb{R}^d$. For almost all $\xi \in \mathbb{R}^r$,

$$|F(w, \xi) - F(w', \xi)| \leq L_0(\xi) \|w - w'\|_2,$$

for all $w, w' \in \mathbb{R}^d$, where $L_0(\xi)$ is a real-valued measurable function which is square integrable, $Q := \mathbb{E}[L_0(\xi)^2] < \infty$. As is common in machine learning applications, we assume that $f(w) \geq 0$ for all $w \in \mathbb{R}^d$ without serious loss of generality, as if $\inf_{w \in \mathbb{R}^d} f(w) \geq -b > -\infty$ for some $b > 0$, $f(w)$ can be redefined as $f(w) := \mathbb{E}[F(w, \xi)] + b$.

Let $m(S)$ denote the Lebesgue measure of any measurable set S . Let $B_\epsilon^p(w) := \{x : \|x - w\|_p \leq \epsilon\}$ and $\overline{B}_\epsilon^p(w) := \{x : \|x - w\|_p \leq \epsilon\}$, for $\epsilon \geq 0$ and $p \geq 1$, and further let $B_\epsilon^p := B_\epsilon^p(0)$ and $\overline{B}_\epsilon^p = \overline{B}_\epsilon^p(0)$.

The Clarke ϵ -subdifferential (Goldstein, 1977) has been defined using the Euclidean norm for a function $g(w)$ as

$$\partial_\epsilon g(w) := \text{co}\{\partial g(x) : x \in \overline{B}_\epsilon^2(w)\},$$

where co denotes the convex hull, and $\partial g(x)$ denotes the Clarke subdifferential, which for a locally Lipschitz continuous function $g(w)$ is equal to

$$\partial g(w) = \text{co}\{v : \exists x^k \rightarrow w, x^k \in D, \nabla g(x^k) \rightarrow v\},$$

where D is the domain of $\nabla g(w)$. The Clarke ϵ -subdifferential is a commonly used relaxation of the Clarke subdifferential for use in the development and analysis of algorithms for the minimization of non-smooth non-convex Lipschitz continuous loss functions, see for example (Davis et al., 2022; Kornowski and Shamir, 2021; Metel, 2022; Zhang et al., 2020). At times it is more convenient to consider different norms, so we define a generalization for $p \geq 1$ as

$$\partial_\epsilon^p g(w) := \text{co}\{\partial g(x) : x \in \overline{B}_\epsilon^p(w)\},$$

and we will also consider a smaller subdifferential, removing the convex hull:

$$\hat{\partial}_\epsilon^p g(w) := \{\partial g(x) : x \in \overline{B}_\epsilon^p(w)\}.$$

Proposition 1. *Let $g(w)$ be a locally Lipschitz continuous function for $w \in \mathbb{R}^d$. For $\epsilon \geq 0$ and $p \geq 1$, $\partial_\epsilon^p g(w)$ and $\hat{\partial}_\epsilon^p g(w)$ are compact and outer semicontinuous for $w \in \mathbb{R}^d$.*

Let $\{\alpha_k\}$ be a sequence such that $\alpha_k > 0$ for all $k \in \mathbb{N}$ with $\lim_{k \rightarrow \infty} \alpha_k = 0$. The next proposition proves the continuous convergence (Rockafellar and Wets, 2009, Definition 5.41) of $\partial_{\alpha_k}^p g(w)$ and $\hat{\partial}_{\alpha_k}^p g(w)$ to $\partial g(w)$.

Proposition 2. *Let $g(w)$ be a locally Lipschitz continuous function for $w \in \mathbb{R}^d$. The set-valued mappings $\partial_{\alpha_k}^p g(w)$ and $\hat{\partial}_{\alpha_k}^p g(w)$ converge continuously to $\partial g(w)$ for all $w \in \mathbb{R}^d$.*

It is not assumed that $f(w)$ nor $F(w, \xi)$ are differentiable. We instead define $\widetilde{\nabla} F(w, \xi)$ to be a Borel measurable function which equals the gradient of $F(w, \xi)$ almost everywhere it exists. This can be computed using back propagation for a wide range of neural network architectures made up of elementary (measurable) functions, see (Bolte and Pauwels, 2020, Proposition 3 & Theorem 2) for more details.

An important concept used in the convergence analysis in Section 5 is the perturbation of weights using samples of a random variable $u : \Omega \rightarrow \mathbb{R}^d$, which is uniformly distributed over $\overline{B}_{\frac{\alpha}{2}}^\infty(w)$ for an $\alpha > 0$, denoted as $u \sim U(\overline{B}_{\frac{\alpha}{2}}^\infty)$. A key benefit of this perturbation is that the expected value of the loss function becomes smooth: the gradient of $f_\alpha(w) := \mathbb{E}[f(w + u)]$ is $L_1^\alpha := 2\alpha^{-1}\sqrt{d}L_0$ -Lipschitz continuous (Metel, 2022, Property 6). We will also need the following proposition.

Proposition 3. *For all $w \in \mathbb{R}^d$ and $\alpha > 0$, it holds that $\nabla f_\alpha(w) \in \partial_{\frac{\alpha}{2}}^\infty f(w)$.*

3 Finite Precision Environments

This section sets the notation for floating and fixed-point arithmetic environments and gives some preliminary results. We will use the notation $\mathbb{F} \subset \mathbb{R}$ to denote a general finite precision environment when further specification is not required. The notation $\mathbb{L} \subset \mathbb{R}$ and $\mathbb{I} \subset \mathbb{R}$ will denote a floating and fixed-point environment, respectively. For $m, n \in \mathbb{Z}$, with $m \leq n$, let $[n]_m := [m, \dots, n]$, and in particular $[n] := [n]_1$.

Following the notation of (Higham, 2002, Chapter 2), a number $y \in \mathbb{L}$ can be represented as

$$y = \pm\beta^e \times .d_1d_2\dots d_t, \tag{2}$$

where \pm is chosen using a sign bit (0 for positive, 1 for negative), $\beta \in \mathbb{Z}_{>1}$ is the base, $t \in \mathbb{Z}_{>0}$ is the number of precision digits, the exponent $e \in [e_{\min}, e_{\max}] \subset \mathbb{Z}$ for $e_{\min} \leq e_{\max} \in \mathbb{Z}$, $d_i \in \mathbb{Z}_{\geq 0}$, and $d_i < \beta$ for $i \in [t]$. To enforce a unique representation, the normalized floating-point numbers \mathbb{L}_N have $d_1 \neq 0$, with $\lambda_N := \beta^{e_{\min}-1}$ being the smallest positive representable number in \mathbb{L}_N .

Following (Gupta et al., 2015), all $y \in \mathbb{I}$ are represented in the form of

$$[e_r e_{r-1}(\dots) e_1 . d_1 d_2(\dots) d_t], \quad (3)$$

written in radix complement (Weik, 2001, Page 1408), using $r \in \mathbb{Z}_{\geq 0}$ digits to represent the integer part and $t \in \mathbb{Z}_{\geq 0}$ digits to represent the fractional part of y , with $r+t > 0$, $0 \leq e_i < \beta$ for all $i \in [r]$, and $0 \leq d_i < \beta$ for all $i \in [t]$, for a base $\beta \in \mathbb{Z}_{>1}$.

For any \mathbb{F} , let Λ^- , λ , and Λ^+ denote the smallest, the smallest positive, and the largest representable numbers, respectively. Their explicit value as well as further background on finite precision environments can be found in Section 9.1. The next proposition verifies that the set of elements representable in floating and fixed-point environments are countable.

Proposition 4. *Let $\widehat{\mathbb{F}} := \{y \in \mathbb{L}_{t,e_{\min}}^{\beta,e_{\max}} : \beta \in \mathbb{Z}_{>1}, t \in \mathbb{Z}_{>0}, \mathbb{Z} \ni e_{\min} \leq e_{\max} \in \mathbb{Z}\} \cup \{y \in \mathbb{I}_{r,t}^{\beta} : \beta \in \mathbb{Z}_{>1}, r \in \mathbb{Z}_{\geq 0}, t \in \mathbb{Z}_{\geq 0}, r+t \in \mathbb{Z}_{>0}\}$ be the set of all elements representable by finite precision environments of the form (2) and (3), where $\mathbb{L}_{t,e_{\min}}^{\beta,e_{\max}}$ denotes an \mathbb{L} in base β with t precision digits and an exponent range of $[e_{\min}, e_{\max}]$, and $\mathbb{I}_{r,t}^{\beta}$ denotes an \mathbb{I} in base β with r integer digits and t fractional digits. It holds that $\widehat{\mathbb{F}} = \mathbb{Q}$.*

To avoid any ambiguity, the range of an \mathbb{F} is defined as the set $\{x \in \mathbb{R} : \Lambda^- \leq x \leq \Lambda^+\}$, whereas the exponent range as used in Proposition 4 can be taken simply as $\{x \in \mathbb{Z} : e_{\min} \leq x \leq e_{\max}\}$. We will consider two forms of rounding: rounding to nearest and stochastic rounding. Given an $x \in \mathbb{R}$ in the range of \mathbb{F} , let $\lfloor x \rfloor_{\mathbb{F}} := \max\{y \in \mathbb{F} : y \leq x\}$ and $\lceil x \rceil_{\mathbb{F}} := \min\{y \in \mathbb{F} : y \geq x\}$, and let $R(x) \in \mathbb{F}$ denote a function which performs one of the two rounding methods. For rounding to nearest,

$$R(x) \in \underset{y \in \{\lfloor x \rfloor_{\mathbb{F}}, \lceil x \rceil_{\mathbb{F}}\}}{\operatorname{argmin}} |y - x|.$$

When $\lceil x \rceil_{\mathbb{F}} - x = x - \lfloor x \rfloor_{\mathbb{F}}$, this work does not depend on the use of a specific tie-breaking rule, but for simplicity we assume that it is deterministic, such as rounding to even or away (IEEE Computer Society, 2019, Section 4.3.1). We note that for odd bases there is no need for tie-breaking rules when rounding to nearest a $y \in \mathbb{F}$ to the same \mathbb{F} with the same β and any t , see Proposition 21 in Section 9.1.

For stochastic rounding,

$$R(x) := \begin{cases} \lceil x \rceil_{\mathbb{F}} & \text{with probability } p = \frac{x - \lfloor x \rfloor_{\mathbb{F}}}{\lceil x \rceil_{\mathbb{F}} - \lfloor x \rfloor_{\mathbb{F}}} \\ \lfloor x \rfloor_{\mathbb{F}} & \text{with probability } 1 - p. \end{cases}$$

If we consider the error $\delta := R(x) - x$, it is well known that $\mathbb{E}[\delta] = 0$, e.g. (Connolly et al., 2021, Lemma 5.1). We will also need a bound on the variance.

Proposition 5. *It holds that*

$$\mathbb{E}[\delta] = 0 \text{ and } \text{Var}(\delta) = \mathbb{E}[\delta^2] \leq \frac{\beta^{2(e-t)}}{4},$$

where e is the exponent of the representation of $\lfloor |x| \rfloor_{\mathbb{F}}$ or $e = 0$, when $\mathbb{F} = \mathbb{L}$ or \mathbb{I} , respectively.

For stochastic rounding in the next proposition, we consider sampling from $U([0, 1])$ to generate the random output, with further details given in the proof.

Proposition 6. *Rounding to nearest and stochastic rounding are Borel measurable functions.*

As is standard (IEEE Computer Society, 2019, Section 5.4), we make the following assumption.

Assumption 7. *The basic operations $\text{op} \in \{+, -, \times, \div\}$ and $\sqrt{\cdot}$ performed on any $y, z \in \mathbb{R}$ ($z \in \mathbb{R}_{\geq 0}$) resulting in $x = y \text{ op } z$ ($x = \sqrt{z}$) is rounded to $R(x)$ as if x was first computed exactly in \mathbb{R} .*

4 Past Work on Optimization with Computational Error

Research on optimization in environments with error is vast when considering stochastic optimization as a subset. The minimization of a stochastic function with further computational error seems to be a topic much less explored. We highlight a few papers which were found to be most relevant to the current research.

An influential paper for this work was (Bertsekas and Tsitsiklis, 2000), where the convergence of a gradient method of the form $w^{k+1} = w^k + \eta^k (s^k + e^k)$ is studied, where η^k is a step-size, s^k is a direction of descent, e^k is a deterministic or stochastic error, and it is assumed that $f(w)$ has a Lipschitz continuous gradient. It was proven that $f(w^k)$ converges, and if the limit is finite, then $\nabla f(w^k) \rightarrow 0$, without any type of boundedness assumptions.

In (Solodov and Zavriev, 1998), a parallel projected incremental algorithm onto a convex compact set is proposed for solving finite-sum problems. It is assumed that there is non-vanishing bounded error when computing the subgradients $g_i(w) \in \partial f_i(w)$ of each subfunction, with a convergence result to an approximate stationary point with an error level relative to the error in computing the subgradients. Each subfunction $f_i(w)$ is assumed to be Lipschitz continuous but regular, i.e. its one-sided directional derivative exists and for all $v \in \mathbb{R}^d$ $f'(w; v) = \max_{g \in \partial f_i(w)} \langle g, v \rangle$ (Clarke, 1990, Section 2.3), which precludes functions with downward cusps such as $(1 - \text{ReLU}(x))^2$ (Davis et al., 2020, Section 1).

Recent work studying the convergence of gradient descent for convex loss functions with a Lipschitz continuous gradient in a low-precision floating-point environment is presented in (Xia et al., 2022). Besides proposing biased stochastic rounding schemes which prevent small gradients from being rounded to zero, inequalities are provided involving the step size, the unit roundoff, and the norms of the gradient and iterates which guarantee either a

convergence rate to the optimal solution, or at least the (expected) monotonicity of the loss function values.

We also mention the paper (Yang et al., 2019), which studies the algorithm $w^{k+1} = R(w^k - \eta^k \nabla \tilde{f}(w^k))$, where $\nabla \tilde{f}(w)$ is a stochastic gradient and $R(\cdot)$ performs stochastic rounding into an \mathbb{L} . It is assumed that the loss function $f(w)$ is strongly convex, with Lipschitz continuous gradient and Hessian, with $\nabla \tilde{f}(w^k)$ being uniformly bounded from $\nabla f(w^k)$ for all $k \geq 1$. Convergence to a neighbourhood of the optimal solution is proven which depends on the precision of \mathbb{L} , with an improved dependence proven when considering an exponential moving average of iterates computed in full-precision.

5 Perturbed SGD with Computational Errors

Given an initial iterate w^1 , we consider a perturbed mini-batch stochastic gradient descent algorithm of the form

$$w^{k+1} = w^k - \frac{\eta_k}{M} \sum_{i=1}^M \widehat{\nabla} F(w^k + \hat{u}^k, \xi^{k,i}, b^{k,i}) + e^k, \quad (4)$$

where $\eta_k \in \mathbb{R}_{>0}$ is the step-size, $M \in \mathbb{Z}_{>0}$ is the mini-batch size, $\hat{u}^k \in \mathbb{R}^d$ is a sample from a probability distribution \widehat{P}_{v^k} , where $v^k \in \mathbb{R}^p$ are the parameters of the distribution, $\{\xi^{k,i}\}$ are M samples of ξ , and $\{b^{k,i}\} \subset \mathbb{R}^s$ are M samples of a random vector $b \in \mathbb{R}^s$ for an $s \in \mathbb{N}$. It is assumed that for all $j \in [s]$, b_j is a discrete uniformly distributed random variable over a finite set $V_j \subset \mathbb{R}$, i.e. $\mathbb{P}(b_j \in V_j) = 1$. A sequence $\{\alpha_k\}_{k \in \mathbb{N}} \subset \mathbb{R}_{>0}$ will play a role in the assumptions placed on $\widehat{\nabla} F(w^k + \hat{u}^k, \xi^{k,i}, b^{k,i})$. This sequence and the random vector e^k will be described later in this section. The sampling of \hat{u}^k , $\{\xi^{k,i}\}$, and $\{b^{k,i}\}$ is assumed to be done independently. We consider three filtrations on the probability space (Ω, \mathcal{F}, P) : $\{\mathcal{F}_k\}$ where $\mathcal{F}_k := \sigma(w^j : j \in [k])$, $\{\mathcal{G}_k\}$ where $\mathcal{G}_k := \sigma(w^j, \hat{u}^j, \{\xi^{j,i}\}, \{b^{j,i}\} : j \in [k])$, and $\{\mathcal{H}_k\}$ where $\mathcal{H}_k := \sigma(w^j, \hat{u}^j, \{\xi^{j,i}\}, \{b^{j,i}\}, e^j : j \in [k])$. We assume that η_k , v_k , and α_k are adapted to either $\{\mathcal{F}_k\}$ or $\{\mathcal{H}_{k-1}\}$ (with $\mathcal{H}_0 := \{\emptyset, \Omega\}$). We note that w^k is \mathcal{H}_{k-1} -measurable, hence $\mathcal{F}_k \subseteq \mathcal{H}_{k-1}$. The motivation to also consider \mathcal{H}_{k-1} instead of simply \mathcal{F}_k is motivated by a step-size which will be presented in Section 6. To streamline the discussion let $\mathcal{I}_k = \mathcal{F}_k$ or \mathcal{H}_{k-1} throughout.

The function $\widehat{\nabla} F(w, \xi, b)$ is an approximation of $\widetilde{\nabla} F(w, \xi)$ subject to errors which are a function of $(w, \xi, b) \in \mathbb{R}^{d+p+s}$. The motivating application is using finite precision arithmetic to approximately compute $\widetilde{\nabla} F(w, \xi)$. The inclusion of the random vector $b \in \mathbb{R}^s$ is to model the use of (approximate) stochastic rounding. The size s of b would then equal the number of basic arithmetic operations required to approximately compute $\widetilde{\nabla} F(w, \xi)$, see (Croci et al., 2022, Section 7) for an overview of the implementation of stochastic rounding in practice. We assume that $\widehat{\nabla} F(w, \xi, b)$ is a Borel measurable function in $(w, \xi, b) \in \mathbb{R}^{d+p+s}$. The following proposition considers the case where $\widehat{\nabla} F(w, \xi, b)$ approximates $\widetilde{\nabla} F(w, \xi)$ at only a countable number of points, such as in a finite precision environment for all $(w, \xi) \in \mathbb{F}^{d+p}$.

Proposition 8. *Assume that $\widehat{\nabla} F(w, \xi, b)$ approximates $\widetilde{\nabla} F(w, \xi)$ at a countable set of points*

$\{w^i, \xi^i\}_{i=1}^\infty \subset \mathbb{R}^{d+p}$. It can be extended into a Borel measurable function in $(w, \xi, b) \in \mathbb{R}^{d+p+s}$ equal to $\widehat{\nabla}F(w, \xi)$ for almost all $(w, \xi) \in \mathbb{R}^{d+p}$.

The error assumptions for $\widehat{\nabla}F(w, \xi, b)$ are of a general form, and are not dependent on specifics such as the number of basic arithmetic operations or the rounding method, which allows the convergence analysis to be applicable for a wide range of computational error.

Assumption 9. *There exists constants $c_1 > 0, c_2 > 0$, and a $\overline{K} \in \mathbb{N}$ such that for all $k \geq \overline{K}$,*

$$\langle \mathbb{E}[\widehat{\nabla}F(w^k + \hat{u}, \xi, b) | \mathcal{I}_k], \nabla f_{\alpha_k}(w^k) \rangle \geq c_1 \|\nabla f_{\alpha_k}(w^k)\|_2^2, \quad (5)$$

and

$$\mathbb{E}[\|\widehat{\nabla}F(w^k + \hat{u}, \xi, b)\|_2^2 | \mathcal{I}_k] \leq c_2 Q, \quad (6)$$

where $\hat{u} \sim \widehat{P}_{v^k}$, $f_{\alpha_k}(w) := \mathbb{E}[f(w + u)]$ for $u \sim U(\overline{B}_{\frac{\alpha_k}{2}}^\infty)$, and recalling that $Q = \mathbb{E}[L_0(\xi)^2]$.

Assuming that $\lim_{k \rightarrow \infty} \alpha_k = 0$, $\overline{K} \in \mathbb{N}$ can be chosen such that (5) is only required to hold for $\alpha_k \leq \overline{\alpha}$ for a chosen $\overline{\alpha} > 0$. These assumptions are variants of classic error assumptions, see (Levitin and Polyak, 1966, Equations (4.3) & (4.4)) and (Bertsekas and Tsitsiklis, 2000, Equation (1.5)), tailored to our problem setting. Equation (5) states that in expectation, $-\widehat{\nabla}F(w^k + \hat{u}, \xi, b)$ must be a direction of descent for f_{α_k} at w^k when $k \in \mathbb{N}$ is sufficiently large. To better understand Assumption 9 we consider the ideal setting where $\widehat{\nabla}F(w, \xi, b) = \widetilde{\nabla}F(w, \xi)$ in the following proposition.

Proposition 10. *For all $w \in \mathbb{R}^d$ and $\alpha > 0$, with $u \sim U(\overline{B}_{\frac{\alpha}{2}}^\infty)$,*

$$\langle \mathbb{E}[\widetilde{\nabla}F(w + u, \xi)], \nabla f_\alpha(w) \rangle \geq \|\nabla f_\alpha(w)\|_2^2, \quad (7)$$

and

$$\mathbb{E}[\|\widetilde{\nabla}F(w + u, \xi)\|_2^2] \leq Q, \quad (8)$$

and in particular, for almost all $w \in \mathbb{R}^d$

$$\mathbb{E}[\|\widetilde{\nabla}F(w, \xi)\|_2^2] \leq Q. \quad (9)$$

When $\widehat{\nabla}F(w, \xi, b) = \widetilde{\nabla}F(w, \xi)$ and $\hat{u} \sim U(\overline{B}_{\frac{\alpha_k}{2}}^\infty)$, Assumption 9 is satisfied with $c_1 = c_2 = 1$ from inequalities (7) and (8). Given that any $0 < c_1 < 1$ and $1 < c_2 < \infty$ are valid, Assumption 9 allows $\widehat{\nabla}F(w, \xi, b)$ to be an approximation of $\widetilde{\nabla}F(w, \xi)$ with nontrivial error, which is only enforced in expectation. Inequality (9) is given to motivate an assumption considered later in this section (see inequality (12)).

Even when $\hat{u} \sim U(\overline{B}_{\frac{\alpha_k}{2}}^\infty)$ and stochastic rounding is used when approximately computing $\widetilde{\nabla}F(w + u, \xi)$, it cannot be assumed in general that $c_1 = 1$, which is highlighted in the next proposition.

Proposition 11. *The expected rounding error from computing batch normalization and its gradient using stochastic rounding is in general non-zero.*

For simplicity let $\widehat{\nabla}F^{k,i}(w^k) := \widehat{\nabla}F(w^k + \hat{u}^k, \xi^{k,i}, b^{k,i})$ for $i \in [M]$, and $\widehat{\nabla}\overline{F}^k(w^k) := \frac{1}{M} \sum_{i=1}^M \widehat{\nabla}F^{k,i}(w^k)$. We will also require the following bound.

Proposition 12. *For all $k \geq \overline{K}$,*

$$\mathbb{E}[\|\widehat{\nabla}\overline{F}^k(w^k)\|_2^2 | \mathcal{I}_k] \leq c_2 Q.$$

The vector $e^k \in \mathbb{R}^d$ is random noise with $\mathbb{E}[e_k | \mathcal{I}_k, \mathcal{G}_k] = 0$.¹ The motivation for adding this error term is to assume that only a finite precision is used when computing (4) given w^k , η_k , M , and $\{\widehat{\nabla}F^{k,i}(w^k)\}$, to model the error from the addition, subtraction, multiplication, and division. The zero-mean assumption can be justified if stochastic rounding is used. Our convergence analysis requires the assumption that $\mathbb{E}[\|e^k\|_2^2 | \mathcal{I}_k] \leq c_3 \eta_k^2$ for some constant $c_3 > 0$. A stronger result holds assuming that the computation is done in an \mathbb{I} with stochastic rounding with no overflow occurring.

Proposition 13. *Assume*

$$w^k \ominus (\eta_k \otimes M) \otimes (\widehat{\nabla}F^{k,1}(w^k) \oplus \dots \oplus \widehat{\nabla}F^{k,M}(w^k)) = w^k - \frac{\eta_k}{M} \sum_{i=1}^M \widehat{\nabla}F^{k,i}(w^k) + e^k, \quad (10)$$

where the “o” symbols represent the corresponding operation in a fixed-point environment $\mathbb{I}_t^\beta \subset \mathbb{R}$ in base $\beta \in \mathbb{Z}_{>0}$, with $t \in \mathbb{Z}_{\geq 0}$ fractional digits using stochastic rounding. Assume that $w^k, \widehat{\nabla}F^{k,i}(w^k) \in (\mathbb{I}_t^\beta)^d$ for $i \in [M]$, and that $\eta_k, M \in \mathbb{I}_t^\beta$. If no overflow occurs in the computation of the left-hand-side of (10), it holds for $c_3 = \frac{M}{4}(Mc_2Q + 1)$ that

$$\mathbb{E}[\|e^k\|_2^2 | \mathcal{I}_k] \leq c_3 \beta^{-2t} \leq c_3 \eta_k^2.$$

We now present the main result of this work.

Theorem 14. *Assume that Perturbed SGD (4) is run such that Assumption 9 holds for a non-increasing α_k for all $k \geq 1$, with $\{\alpha_k\}$ and $\{\eta_k\}$ chosen such that*

$$\sum_{k=1}^{\infty} \alpha_k^d \eta_k = \infty \text{ and } \sum_{k=1}^{\infty} \alpha_k^{d-1} \eta_k^2 < \infty$$

almost surely, $\lim_{k \rightarrow \infty} \alpha_k = 0$, and that there exists a constant $c_3 > 0$ such that $\mathbb{E}[\|e^k\|_2^2 | \mathcal{I}_k] \leq c_3 \eta_k^2$ for all $k \geq 1$. Almost surely, there exists a subsequence of indices $\{k_i\}$ such that

$$\lim_{i \rightarrow \infty} \|\nabla f_{\alpha_{k_i}}(w^{k_i})\|_2 = 0$$

and for every accumulation point w^ of $\{w^{k_i}\}$, it holds that*

$$\text{dist}(0, \partial f(w^*)) = 0.$$

¹When $\mathcal{I}_k = \mathcal{F}_k$ this simplifies to $\mathbb{E}[e_k | \mathcal{G}_k] = 0$ given that $\mathcal{F}_k \subseteq \mathcal{G}_k$.

The next proposition gives a family of sequences $\{\alpha_k\}$ and $\{\eta_k\}$ which satisfy the conditions of Theorem 14.

Proposition 15. *For $0.5 < q < 1$ and $p = \frac{(1-q)}{d}$, set $\alpha_k = \frac{1}{k^p}$ and $\hat{\eta}_k = \frac{1}{k^q}$ for $k \geq 1$. Let $\{\psi_k\}_{k=1}^\infty \subset \mathbb{R}$ be a sequence of \mathcal{I}_k -measurable random variables with essential supremum $\Psi^S < \infty$ and infimum $\Psi^I > 0$, i.e. $\mathbb{P}(\Psi^I \leq \psi_k \leq \Psi^S) = 1$ for all $k \geq 1$. Setting $\eta_k = \psi_k \hat{\eta}_k$ for $k \geq 1$, it holds that $\{\alpha_k\}$ and $\{\eta_k\}$ satisfy the conditions of Theorem 14.*

Using PSGD with $\lim_{k \rightarrow \infty} \alpha_k = 0$ has the appealing property of optimizing a sequence of approximating functions $\{f_{\alpha_k}(w)\}_{k=1}^\infty$ which are converging to the true function $f(w)$ (Metel, 2022, Proposition 5.2). The following corollary considers a fixed $\alpha_k = \alpha > 0$ in order to prove a non-asymptotic convergence bound in expectation for the L_∞ -norm Clarke $\frac{\alpha}{2}$ -subdifferential.

Corollary 16. *Assume that Perturbed SGD (4) is run for $\hat{k} \sim U([K])$ iterations uniformly sampled over $[K]$, with $\alpha_k = \alpha > 0$, $\eta_k = \frac{\tau}{\sqrt{K}}$ for $\tau > 0$, Assumption 9 holds with $\bar{K} = 1$, and that there exists a constant $c_3 > 0$ such that $\mathbb{E}[\|e^k\|_2^2 | \mathcal{I}_k] \leq c_3 \eta_k^2$ for all $k \in [K]$. It holds that*

$$\mathbb{E}[\text{dist}(0, \partial_{\frac{\alpha}{2}}^\infty f(\hat{w}))^2] \leq \frac{f_\alpha(w^1)}{\tau c_1 \sqrt{K}} + \frac{\sqrt{d} L_0 \tau}{\alpha c_1 \sqrt{K}} (c_2 Q + c_3).$$

Giving an asymptotic convergence result in Theorem 14 in a setting motivated by finite precision arithmetic may seem contradictory, in particular requiring that $\lim_{k \rightarrow \infty} \alpha_k = 0$. If we consider a sequence of environments $\{\mathbb{F}_{t_j}\}_{j=1}^\infty$ with precision/fractional digits satisfying $0 < t_j < t_{j+1}$ for all $j \in \mathbb{N}$, then sequences of PSGD can be generated satisfying the requirements of Theorem 14 by moving to precision t_{j+1} when the convergence requirements can no longer be supported using precision t_j . This idea was successfully used in (Gupta et al., 2015, Figure 3) where neural network training in \mathbb{I} was performed with $t = 12$ until stagnation occurred, after which the fractional digits were increased to $t = 16$ resulting in a rapid accuracy improvement.

5.1 Choice of \hat{P}_{v^k}

If (5) were to hold, the simplest choice for \hat{P}_{v^k} would be a degenerate distribution with $\mathbb{P}(\hat{u}^k = 0) = 1$, with (4) simplifying to an implementation of SGD. Assuming this is not the case, Proposition 10 motivates the choice of $\hat{P}_{v^k} = U(\bar{B}_{\frac{\alpha}{2}}^\infty)$. The assumption of sampling $\hat{u} \sim U(\bar{B}_{\frac{\alpha}{2}}^\infty)$ is not compatible with finite precision arithmetic though, so we will now study its approximation.

For the remainder of this section we will consider a sequence of finite-precision environments $\{\mathbb{F}_{t_j}\}_{j=1}^\infty$ which have a fixed β , r , or pair (e_{min}, e_{max}) , but increasing t . We assume that $\bar{B}_{\frac{\alpha}{2}}^\infty$ for a chosen $\alpha > 0$ is contained in the range $[\Lambda^-, \Lambda^+]^d$ of the d -dimensional finite precision environment $\mathbb{F}_{t_1}^d$.² We denote by $R_{t_j}(\cdot) : \mathbb{R}^v \rightarrow \mathbb{F}_{t_j}^v$ rounding to nearest into $\mathbb{F}_{t_j}^v$ for $v = 1$ or d .

²This implies that $\bar{B}_{\frac{\alpha}{2}}^\infty$ is contained in the range of $\mathbb{F}_{t_j}^d$ for all $j \geq 1$.

Assume there exists a random number generator which can output samples of a discrete random variable \hat{u}_{t_j} taking on values $\{\hat{u}_{t_j}^k\} \subset \mathbb{F}_{t_j}^d$, and that the probability $\mathbb{P}(\hat{u}_{t_j} = \hat{u}_{t_j}^k) = \mathbb{P}(R_{t_j}(u) = \hat{u}_{t_j}^k)$ for $u \sim U(\overline{B}_{\frac{\alpha}{2}}^\infty)$. It is convenient to model the random number generator as receiving a sample of u which it then rounds to $R_{t_j}(u)$ to generate a sample of \hat{u}_{t_j} instead of considering a deterministic method such as with pseudorandom number generators. In general $\{\hat{u}_{t_j}^k\} \not\subset \overline{B}_{\frac{\alpha}{2}}^\infty$, i.e., u can be rounded outside of $\overline{B}_{\frac{\alpha}{2}}^\infty$. We will assume that $\frac{\alpha}{2} \in \mathbb{F}_{t_1}$, from which it holds that $\{\hat{u}_{t_j}^k\} \subset \overline{B}_{\frac{\alpha}{2}}^\infty$ for all $j \geq 1$ by the monotonicity of rounding to nearest (Higham, 2002, Page 38), matching the typical behaviour of a random number generator, which is without much loss of generality as t_1 can be chosen arbitrarily large in the next theorem.

Assumption 9 was chosen to fit with sequences generated by PSGD (4) for general $\{\hat{P}_{v^k}\}$ including discrete distributions. For the next theorem, which considers sampling from $u \sim U(\overline{B}_{\frac{\alpha}{2}}^\infty)$, we consider the following assumptions on $\widehat{\nabla}F(w, \xi, b)$ which can be seen as direct relaxations of equations (7) and (9).

Assumption 17. *For a chosen $\alpha > 0$, there exists constants $c_1 > 0$ and $c_2 > 0$ such that for all $w \in \mathbb{R}^d$,*

$$\langle \mathbb{E}[\widehat{\nabla}F(w + u, \xi, b)], \nabla f_\alpha(w) \rangle \geq c_1 \|\nabla f_\alpha(w)\|_2^2, \quad (11)$$

and for almost all $w \in \mathbb{R}^d$,

$$\mathbb{E}[\|\widehat{\nabla}F(w, \xi, b)\|_2^2] \leq c_2 Q, \quad (12)$$

where $u \sim U(\overline{B}_{\frac{\alpha}{2}}^\infty)$ and $f_\alpha(w) := \mathbb{E}[f(w + u)]$.

If Assumption 17 holds, the following theorem proves that when a discretized approximation of u is used, as t is increased, (11) holds almost everywhere in the limit.

Theorem 18. *Assume that $u \sim U(\overline{B}_{\frac{\alpha}{2}}^\infty)$ for $\frac{\alpha}{2} \in \mathbb{F}_{t_1}$ and that Assumption 17 holds for $\alpha > 0$. For almost all $w \in \mathbb{R}^d$,*

$$\lim_{j \rightarrow \infty} \mathbb{E}[\widehat{\nabla}F(w + R_{t_j}(u), \xi, b) - \widehat{\nabla}F(w + u, \xi, b)] = 0,$$

and in particular, for almost all $w \in \mathbb{R}^d$,

$$\lim_{j \rightarrow \infty} \langle \mathbb{E}[\widehat{\nabla}F(w + R_{t_j}(u), \xi, b)], \nabla f_\alpha(w) \rangle \geq c_1 \|\nabla f_\alpha(w)\|_2^2.$$

6 Empirical Analysis of SGD Variants in Low-Precision Environments

This section compares different variants of SGD to improve the test set accuracy for image recognition tasks in low-precision arithmetic environments. The focus is on two Resnet models: Resnet 20 trained on CIFAR-10 (R20C10) and Resnet 32 trained on CIFAR-100 (R32C100). The experiments were conducted using QPyTorch (Zhang et al., 2019b), which

enabled the simulation of training using floating and fixed-point arithmetic with rounding to nearest and stochastic rounding. For all experiments we train for 200 epochs, with an initial SGD step-size of $\hat{\eta}_k = 0.1$ (before rounding), which is divided by 10 after 100 epochs, with a mini-batch size of $M = 128$. The plots are always of the mean (thick solid line), minimum (thin solid line), and maximum (dotted line) test set accuracy for each epoch over 10 runs. The tested algorithms generally achieve a reasonable level of convergence after the step-size decrease after epoch 100. As the choice of 200 epochs is arbitrary, to avoid any ambiguity, accuracy will be measured as the average accuracy in the last 30 epochs.

Let FLXR denote a floating-point environment with X total bits and 5 exponent bits, following IEEE binary 16 (IEEE Computer Society, 2019, Table 3.5), using rounding to nearest (R = N) or stochastic rounding (R = S). Let FIX/YR denote a fixed-point environment where X is the total number of digits and Y is the number of fractional digits. Our use of QPyTorch followed closely the CIFAR10 Low Precision Training Example found at (Zhang et al., 2019a), which uses FL8³ and FL16. Assuming the training is done in FL8N, we will describe the changes made to the example in our implementation: all weight, gradient, and momentum quantization was done using FL8N, rounding to nearest was used throughout, no gradient accumulator was used, no gradient scaling was performed, and input parameters $\hat{\eta}_k$ and α_k were quantized. In order to do experiments in other environments, the only changes made was the choice of \mathbb{F} and the type of rounding $R(\cdot)$.

The initial focus was to determine a baseline SGD model to do experiments with. Training R20C10, momentum and weight decay were tested in FL8N and FL16N. Plain SGD was chosen as the baseline SGD model given its significantly better performance in FL8N, see Section 11.1 for more details. Given the large rounding error when training in FL8N, significant variation in accuracy can be observed over the 10 runs, summarized by the minimum and maximum accuracies. In all experiments we will not only consider the mean accuracy, but also the minimum accuracy of algorithms, placing value on their ability to return solutions which are close to or above their mean accuracy.

6.1 Gradient Normalization

A simple variant that was found to improve test set accuracy was gradient normalization (GN) as presented in Algorithm 1, where $\mu \in \mathbb{F}_{>0}$ is a small positive constant to avoid division by 0, such as the minimum positive element in \mathbb{F} , $R(\cdot)$ performs the desired rounding scheme, and $\{\hat{\eta}_k\}_{k=1}^{\infty}$ is a baseline step-size sequence.⁴ Experiments were done to compare different variants of GN using the $L2$ instead of $L1$ -norm, as well as using an exponential moving average (EMA) with weight parameter $\beta = R(0.1)$, see the left-hand-side of (13), instead of the simple moving average (SMA) with $q = 10$, which is plotted in Figure 3 in Section 11.2, where SGD with GN is referred to as NSGD and μ was set to λ as suggested. In terms of mean and minimum accuracies, all NSGD variants outperformed SGD, with NSGD using the $L1$ -norm and an SMA (L1,SMA) dominating the other variants, with its mean accuracy being equal to if not greater than the maximum accuracies of the (L1,EMA) and (L2,SMA)

³The number of exponent bits equals 2. This does not include the hidden bit, so in the representation of equation (2), $t = 3$, but d_1 is not required to be stored in memory.

⁴When $k = 1$, η_1 is set to $\hat{\eta}_1$.

Table 1: Mean value of η_k for different variants of GN.

$\hat{\eta}_k = 0.09375$	(L1,SMA)	(L2,SMA)
mean(η_k)	0.09753	0.09520
	(L1,EMA)	(L2,EMA)
mean(η_k)	0.12117	0.15317

variants, with its minimum accuracy being similar to the mean accuracy of the (L2,EMA) variant.

Algorithm 1 GN: Gradient Normalization (by step-size update for iteration $k > 1$)

Input: $\widehat{\nabla}\overline{F}(w^k) \in \mathbb{F}^d$; $\{g_{nrm}^i\}_{i=\max(1,k-q)}^{k-1} \in \mathbb{F}^{\min(k-1,q)}$; $\hat{\eta}_k, \mu \in \mathbb{F}_{>0}$

$g_{nrm}^k = \max(R(\|\widehat{\nabla}\overline{F}(w^k)\|_1), \mu)$
 $m_{ave}^{k-1} = R\left(\frac{1}{\min(k-1,q)} \sum_{i=\max(1,k-q)}^{k-1} g_{nrm}^i\right)$

Output: $\eta_k = R(\hat{\eta}_k * m_{ave}^{k-1} / g_{nrm}^k)$

If the norm of the gradient is larger (smaller) than average, then the step-size $\hat{\eta}_k$ is decreased (increased). With NSGD, we expect that the values of $\{\eta_k\}$ will be close to $\{\hat{\eta}_k\}$ on average. For the more common form of NSGD, $\eta_k = R(\hat{\eta}_k / g_{nrm}^k)$ (Shor, 1998, Equation (2.7), Nesterov, 2004, Section 3.2.3), it seems unclear how to choose $\hat{\eta}_k$ a priori, whereas with NSGD, assuming that $\text{mean}(\eta_k - \hat{\eta}_k) \approx 0$, the need to tune $\{\hat{\eta}_k\}$ is avoided, as for any training task, $\{\hat{\eta}_k\}$ can be set to what has previously been found to be a good step-size schedule for SGD, which also allows for a clearer comparison between SGD with and without normalization.

In the experiments plotted in Figure 3 in Section 11.2, for the first 100 epochs $\hat{\eta}_k = R(0.1) = 0.09375$. The mean value of η_k was computed over all steps in the first 100 epochs over the 10 runs, recorded in Table 1. It can be observed that for all cases $\text{mean}(\eta_k) > 0.09375$. For a successful training algorithm, the gradient norms will start out being relatively large and then decrease on average as the algorithm (hopefully) approaches a stationary point, so that on average the current gradient norm is smaller than previous ones, which could explain why the average step-sizes are larger than $\hat{\eta}_k$. Using an SMA, the bias is quite small compared to using an EMA, for which the upward bias seems to be exacerbated by its “stickiness” in low precision, in the sense that

$$R((1 - \beta)m_{ave}^{k-1} + \beta g_{nrm}^k) = m_{ave}^{k-1} \quad (13)$$

can hold for a wide range of values. For example, if $g_{nrm}^k = 2$ and $1 \leq m_{ave}^{k-1} \leq 7$ with $\beta = R(0.1)$ in FL8N, then (13) holds.

In our implementation of GN, only one rounding operation is performed in each step. This implicitly assumes that intermediate steps are stored in sufficiently high precision such that no additional rounding errors are observable in the final low-precision output. This choice is consistent with the implementation of rounding using QPyTorch, where a quantization layer is added after each layer which induces rounding errors. If this assumption does not

hold, it may be possible to devise rounding aware approximations which reduce the overall error after rounding, see for example (Wang et al., 2022, Section 3.5) where a Taylor series is used to approximately compute the gradient of cross entropy loss for use in low-precision fixed-point training.

Step sizes $\{\eta_k\}$ using GN are not \mathcal{I}_k -measurable but \mathcal{H}_k -measurable.⁵ In an attempt to bridge the gap from the assumptions of Section 5, we propose Delayed GN (DGN), which simply replaces g_{nrm}^k with g_{nrm}^{k-1} , i.e. $\eta_k = R(\hat{\eta}_k * m_{ave}^{k-1}/g_{nrm}^{k-1})$, which is then \mathcal{H}_{k-1} -measurable. If we assume that the gradient magnitudes $\|\widehat{\nabla}F(w^k)\|_1$ and $\|\widehat{\nabla}F(w^{k-1})\|_1$ are positively correlated, then DGN could still possess the benefits of GN in terms of stabilizing the gradient norms. The following proposition gives conditions such that DGN implicitly generates a sequence $\{\psi_k\}$ satisfying the conditions of Proposition 15 in \mathbb{L} using rounding to nearest or stochastic rounding. We will refer to SGD using DGN as DNSGD.

Proposition 19. *Assume that $\mathbb{F} = \mathbb{L}$, $t > 1$, there exists a $\Psi \in \mathbb{F}_{\geq \mu}$ such that $\mathbb{P}(R(\|\widehat{\nabla}F(w^k)\|_1) \leq \Psi) = 1$ for all $k \geq 1$, and that $\hat{\eta}_k \frac{\mu}{\Psi}, \hat{\eta}_k \frac{\Psi}{\mu} \in [\lambda_N, \Lambda^+]$ (the range of \mathbb{L}_N) for all $k \geq 1$. The step-size η_k using DGN can be written as $\eta_k = \psi_k \hat{\eta}_k$ for which there exists a Ψ^I and Ψ^S such that $\mathbb{P}(\Psi^I \leq \psi_k \leq \Psi^S) = 1$.*

6.2 Training in Low-Precision Environments

We now compare the performance of SGD, NSGD, DNSGD, PSGD, PNSGD, and PDNSGD, where PSGD, PNSGD, and PDNSGD are SGD, NSGD, and DNSGD with iterate perturbation. For the perturbed algorithms, the perturbation level was always kept at $\alpha_k = 0.1\hat{\eta}_k$, with the low-precision forward and back propagation computed at $w^k + u^k$ for $u^k = R(u)$, where $u \sim U(\overline{B}_{R(\frac{\alpha_k}{2})}^\infty)$.

We group the experiments into four categories: fixed-point with rounding to nearest, fixed-point with stochastic rounding, floating-point with rounding to nearest, and floating-point with stochastic rounding. Three different methods of ranking algorithms were used. The first method, Sum of Accuracies (SoA), summed each algorithm’s mean and minimum accuracies over each category’s experiments. The second, Sum of Relative Accuracies (SoR), summed each algorithm’s relative accuracies, which were computed by dividing each algorithm’s mean (minimum) accuracy by the highest mean (minimum) accuracy of each experiment. The third method, Sum of Scores (SoS) is a method we propose to overcome shortcomings found with the former two, described in the following section. Each experiment conducted, the resulting accuracies, relative accuracies, and scores of each algorithm, with the SoA, SoR, and SoS rankings for each category of experiments are presented in Tables 2 (all fixed-point experiments), 3 (floating-point rounding to nearest experiments), and 4 (floating-point stochastic rounding experiments) in Section 11.4. It was generally too difficult to interpret a plot of all 6 algorithms, so for each experiment, a maximum of three algorithms were plotted in the following priority: SGD, the algorithm with the highest mean accuracy, the highest minimum accuracy, the lowest mean accuracy, and the lowest minimum accuracy, which are found in Figures 4, 5, and 6 in Section 11.4.

⁵This is assuming that $\{\hat{\eta}_k\}$ are \mathcal{H}_{k-1} -measurable, if instead they are \mathcal{F}_k -measurable or simply deterministic, then $\{\eta_k\}$ are \mathcal{G}^k -measurable.

6.2.1 Sum of Scores

To prevent algorithms from being deemed superior or inferior over trivial differences in accuracy, algorithms are considered to have equal performance, in principle, when the difference in their accuracies is less than $\chi = 0.5\%$. This was implemented using hierarchical clustering to partition the algorithms in each experiment: algorithms’ accuracies are initially placed in their own subsets, $\{p_i\}_{i=1}^6$. The dissimilarity between subsets is measured as

$$\Delta(p_i, p_j) := \max_{a \in p_i, a' \in p_j} |a - a'|, \tag{14}$$

where a and a' are accuracies of algorithms in subsets p_i and p_j . If there are at least two subsets with $\Delta(p_i, p_j) < \chi$, the pair of subsets with the smallest $\Delta(p_i, p_j)$ are combined together. This is repeated until $\Delta(p_i, p_j) \geq \chi$ for all subsets with $i \neq j$. Using the criterion (14) ensures that all algorithms whose accuracies are placed in the same subset p_i have a difference of accuracy less than χ , and are then considered as having the same ranking for the given experiment.

In order to rank the performance of algorithms over multiple experiments, scores equal to $\{5, 3, 1, -1, -3, -5\}$ are given starting from the algorithm with the highest to the lowest accuracy, with the average score given to algorithms in the same subset. These scores were chosen since they are symmetrical, evenly spaced, and results in all averaged scores remaining integer valued. The motivation to weight each experiment equally, by awarding fixed scores, is for our findings to be more robust to our choice of experiments: an algorithm may perform exceptionally well or bad relative to the other algorithms for a particular choice of neural network architecture, data set, and number format, skewing the overall rankings when using SoA or SoR, but this exceptional performance may not be representative over all potential experiments for the given category. With SoS, we limit the influence of any single experiment on the overall rankings.

6.2.2 Training in Low-Bit Fixed-Point Environments

Neural network training in fixed-point environments is of greater practical interest given the simpler arithmetic, resulting in reduced hardware complexity and energy consumption, see (Wang et al., 2022, Table 2), so we will begin with these experiments. In trying to determine the appropriate ratio of fractional bits, we were guided by the results of (Gupta et al., 2015), and experimented with a majority of bits being fractional, given that in their experiments with FI16, the best accuracy occurred with $Y=14$, with further improvement using FI20/16S (Gupta et al., 2015, Figures 1, 2, & 3). The choice of each fixed-point environment FIX/YR was determined by finding the smallest X for which all algorithms did not eventually collapse to random guessing.

The experimental results are given in Table 2 in Section 11.4. For the fixed-point rounding to nearest experiments, the differentiating factor was whether perturbation was used or not. All of the perturbed and non-perturbed algorithms received the same score, respectively. The top two plots in Figure 4 in Section 11.4 are of these experiments, where the mean accuracies of SGD are difficult to see given that they are almost identical to DNSGD and NSGD. The mean accuracies have a cascading waterfall appearance from single runs collapsing at different

epochs. This instability from using rounding to nearest can also be observed in (Gupta et al., 2015, Figure 3), with the training and test set error increasing out of the plot. Considering all methods of ranking, PDNSGD would be considered the best algorithm. Given the almost identical performance of the perturbed algorithms though, PSGD could also be considered the best given that gradient normalization is not required, making it more computationally efficient.

For the fixed-point stochastic rounding experiments, PNSGD is the best performing algorithm according to all methods of ranking. SoA and SoR deemed SGD as the worst performing algorithm, whereas SoS ranked PSGD as the worst. SGD tied for the best mean accuracy in the first experiment, whereas PSGD always had a below average (negative) score in each experiment.

6.2.3 Training in Low-Bit Floating-Point Environments

Following the halving of bits from single to half precision, our initial choice was to try FL8 for our floating-point experiments with rounding to nearest and stochastic rounding. Although using FL8 and FL9⁶ for our R20C10 and R32C100 experiments allowed for a fairly clear comparison between the different algorithms, the maximum test set accuracies achievable of all algorithms were substantially lower than with single precision, and evidence of overfitting was also visible. To give more credence to the results, another set of experiments were done, where for each initial experiment, another mantissa bit was added to increase the overall accuracy, or weight decay was added when there was evidence of overfitting, for a total of 8 floating-point experiments. We note that the additional 4 experiments did not change the best algorithm determined by any of the methods of ranking based on the original 4 experiments, so these additional experiments simply reinforce our initial findings.

Table 3 and Figure 5 in Section 11.4 contain and plot the experimental results for the floating-point rounding to nearest experiments, where the initial experiments of training R20C10 in FL8N and R32C100 in FL9N were augmented with experiments training R20C10 in FL9N, and R32C100 in FL10N. In this setting iterate perturbation seems to have a detrimental effect, with all non-perturbed variants outperforming the perturbed variants. All methods of ranking agree that NSGD is the best performing with PSGD being the worst. There is strong evidence of the benefit of gradient normalization, not only in how NSGD performed best overall, but for all methods of ranking NSGD>DNSGD>SGD and PNSGD>DNSGD>PSGD. Even in the perturbed case, GN performed best, with both perturbed and non-perturbed DGN performing better than having no gradient normalization at all.

Table 4 and Figure 6 in Section 11.4 contain and plot the experimental results for the floating-point stochastic rounding experiments, where the initial experiments of training R20C10 in FL8S and R32C100 in FL9S were augmented with experiments using weight decay equal to $R(1e - 4)$, given the apparent overfitting of the models by all algorithms. With an inverted result compared to the floating-point rounding to nearest experiments, with stochastic rounding, all algorithms using iterate perturbation outperformed the algorithms

⁶Initial training of R32C100 in FL8N with SGD had a test set accuracy of approximately 2%, so the mantissa was increased by one bit in the initial experiments.

without, with PNSGD performing best according to all methods of ranking. According to SoR and SoS, NSGD performed the worst in this set of experiments, with SGD performing the worst according to SoA.

6.2.4 Summary of Results

Based on the three methods of ranking, the algorithms which were found to perform best were PDNSGD for fixed-point rounding to nearest, PNSGD for fixed-point stochastic rounding, NSGD for floating-point rounding to nearest, and PNSGD for floating-point stochastic rounding environments. Of all methods, PNSGD seems to be the most promising algorithm for future use given that it dominated in the experiments using stochastic rounding, which is the rounding method of choice for low-precision deep learning (Gupta et al., 2015; Wang et al., 2022; Yang et al., 2019).

7 Conclusion

This paper studied the theoretical and empirical convergence of variants of SGD with computational error. A new asymptotic convergence result to a Clarke stationary point was presented for Perturbed SGD applied to a stochastic Lipschitz continuous loss function with error in computing its stochastic gradient, as well as the SGD step itself. Variants of SGD using gradient normalization and iterate perturbation were compared empirically to SGD in low-precision floating and fixed-point environments using rounding to nearest and stochastic rounding. In each case, variants were found to have improved test set accuracy compared to SGD, in particular PNSGD for experiments using stochastic rounding.

References

- Dimitri P. Bertsekas and John N. Tsitsiklis. Gradient Convergence in Gradient Methods with Errors. *SIAM Journal on Optimization*, 10(3):627–642, 2000.
- Jérôme Bolte and Edouard Pauwels. A mathematical model for automatic differentiation in machine learning. In H. Larochelle, M. Ranzato, R. Hadsell, M.F. Balcan, and H. Lin, editors, *Advances in Neural Information Processing Systems*, pages 10809–10819. Curran Associates, Inc., 2020.
- Frank H. Clarke. *Optimization and Nonsmooth Analysis*. SIAM, 1990.
- Michael P. Connolly, Nicholas J. Higham, and Theo Mary. Stochastic Rounding and Its Probabilistic Backward Error Analysis. *SIAM Journal on Scientific Computing*, 43(1): A566–A585, 2021.
- Matteo Croci, Massimiliano Fasi, Nicholas J. Higham, Theo Mary, and Mantas Mikaitis. Stochastic rounding: implementation, error analysis and applications. *Royal Society Open Science*, 9(3):211631, 2022.

- Damek Davis, Dmitriy Drusvyatskiy, Sham Kakade, and Jason D. Lee. Stochastic subgradient method converges on tame functions. *Foundations of Computational Mathematics*, 20(1):119–154, 2020.
- Damek Davis, Dmitriy Drusvyatskiy, Yin Tat Lee, Swati Padmanabhan, and Guanghao Ye. A gradient sampling method with complexity guarantees for Lipschitz functions in high and low dimensions. *arXiv preprint arXiv:2112.06969*, 2022.
- Gerald B. Folland. *Real Analysis: Modern Techniques and Their Applications*. Wiley, 1999.
- A.A. Goldstein. Optimization of Lipschitz continuous functions. *Mathematical Programming*, 13(1):14–22, 1977.
- Suyog Gupta, Ankur Agrawal, Kailash Gopalakrishnan, and Pritish Narayanan. Deep Learning with Limited Numerical Precision. In Francis Bach and David Blei, editors, *International Conference on Machine Learning*, pages 1737–1746. PMLR, 2015.
- Kaiming He, Xiangyu Zhang, Shaoqing Ren, and Jian Sun. Deep Residual Learning for Image Recognition. In *Proceedings of the IEEE Conference on Computer Vision and Pattern Recognition*, pages 770–778, 2016.
- Nicholas J. Higham. *Accuracy and Stability of Numerical Algorithms*. SIAM, 2002.
- IEEE Computer Society. IEEE Standard for Floating-Point Arithmetic. *IEEE Std 754-2019 (Revision of IEEE 754-2008)*, pages 1–84, 2019.
- Sergey Ioffe and Christian Szegedy. Batch Normalization: Accelerating Deep Network Training by Reducing Internal Covariate Shift. In Francis Bach and David Blei, editors, *International Conference on Machine Learning*, pages 448–456. PMLR, 2015.
- Guy Kornowski and Ohad Shamir. Oracle Complexity in Nonsmooth Nonconvex Optimization. In M. Ranzato, A. Beygelzimer, Y. Dauphin, P.S. Liang, and J. Wortman Vaughan, editors, *Advances in Neural Information Processing Systems*, pages 324–334. Curran Associates, Inc., 2021.
- Evgeny S. Levitin and Boris T. Polyak. Constrained Minimization Methods. *USSR Computational Mathematics and Mathematical Physics*, 6(5):1–50, 1966.
- Michael R. Metel. Sparse Training with Lipschitz Continuous Loss Functions and a Weighted Group L0-norm Constraint. *arXiv preprint arXiv:2202.06141*, 2022.
- Michael R. Metel and Akiko Takeda. Perturbed Iterate SGD for Lipschitz Continuous Loss Functions. *Journal of Optimization Theory and Applications*, 2022. doi: <https://doi.org/10.1007/s10957-022-02093-0>. Online First.
- Yurii Nesterov. *Introductory Lectures on Convex Optimization: A Basic Course*. Springer Science+Business Media, 2004.

- Herbert Robbins and David Siegmund. A Convergence Theorem for Non Negative Almost Supermartingales and Some Applications. In Jagdish S. Rustagi, editor, *Optimizing Methods in Statistics*, pages 233–257. Elsevier, 1971.
- R. Tyrrell Rockafellar and Roger J-B Wets. *Variational Analysis*. Springer, 2009.
- Rolf Schneider. *Convex Bodies: The Brunn-Minkowski Theory*. Cambridge University Press, 2014.
- Naum Z. Shor. *Nondifferentiable Optimization and Polynomial Problems*. Springer, 1998.
- M. V. Solodov and S. K. Zavriev. Error Stability Properties of Generalized Gradient-Type Algorithms. *Journal of Optimization Theory and Applications*, 98(3):663–680, 1998.
- Maolin Wang, Seyedramin Rasoulinezhad, Philip HW Leong, and Hayden K-H So. NITI: Training Integer Neural Networks Using Integer-Only Arithmetic. *IEEE Transactions on Parallel and Distributed Systems*, 33(11):3249–3261, 2022.
- Martin H. Weik. *Computer Science and Communications Dictionary*. 2001.
- J.H. Wilkinson. *Rounding Errors in Algebraic Processes*. Prentice-Hall, 1965.
- Lu Xia, Stefano Massei, Michiel Hochstenbach, and Barry Koren. On the influence of round-off errors on the convergence of the gradient descent method with low-precision floating-point computation. *arXiv preprint arXiv:2202.12276*, 2022.
- Guandao Yang, Tianyi Zhang, Polina Kirichenko, Junwen Bai, Andrew Gordon Wilson, and Chris De Sa. SWALP: Stochastic Weight Averaging in Low-Precision Training. In Kamalika Chaudhuri and Ruslan Salakhutdinov, editors, *International Conference on Machine Learning*, pages 7015–7024. PMLR, 2019.
- Jingzhao Zhang, Hongzhou Lin, Stefanie Jegelka, Suvrit Sra, and Ali Jadbabaie. Complexity of Finding Stationary Points of Nonconvex Nonsmooth Functions. In Hal Daumé III and Aarti Singh, editors, *International Conference on Machine Learning*, pages 11173–11182. PMLR, 2020.
- Tianyi Zhang, Zhiqiu Lin, Guandao Yang, and Christopher De Sa. QPyTorch’s documentation. <https://qpytorch.readthedocs.io>, 2019a. Accessed: 2022-09-29.
- Tianyi Zhang, Zhiqiu Lin, Guandao Yang, and Christopher De Sa. QPyTorch: A Low-Precision Arithmetic Simulation Framework. In *2019 Fifth Workshop on Energy Efficient Machine Learning and Cognitive Computing - NeurIPS Edition (EMC2-NIPS)*, pages 10–13. IEEE, 2019b.

Appendix

8 Proofs of Sections 2

Proof. (Proposition 1): Let \mathcal{N}_ϵ be a neighbourhood of the set $\overline{B}_\epsilon^p(w)$, with L_ϵ being a Lipschitz constant of $g(x)$ restricted to \mathcal{N}_ϵ . Given that $\|\xi\|_2 \leq L_\epsilon$ for all $\xi \in \partial g(x)$, for all $x \in \overline{B}_\epsilon^p(w)$ (Clarke, 1990, Proposition 2.1.2 (a)), the set $\hat{\partial}_\epsilon^p g(w)$ is bounded. Since $\partial g(w)$ is outer semicontinuous (Clarke, 1990, Proposition 2.1.5 (d)), $\partial g(C)$ is closed if C is compact (Rockafellar and Wets, 2009, Theorem 5.25 (a)), hence $\hat{\partial}_\epsilon^p g(w) = g(\overline{B}_\epsilon^p(w))$ is compact. Since the convex hull of a compact set is compact (Rockafellar and Wets, 2009, Corollary 2.30), it also holds that $\partial_\epsilon^p g(w)$ is compact.

We next prove that $\hat{\partial}_\epsilon^p g(w)$ is outer semicontinuous following (Rockafellar and Wets, 2009, Definition 5.4). Let $w^k \rightarrow w$ and $u^k \rightarrow u$, with $u^k \in \hat{\partial}_\epsilon^p g(w^k)$. There exists at least one $y^k \in \overline{B}_\epsilon^p(w^k)$ such that $u^k \in \partial g(y^k)$. We can assume $\{w^k\}$ is bounded, implying that $\{y^k\}$ is as well. There then exists a subsequence $\{y^{k_i}\}$ which converges to a value y . Let the sequences $\{w^k\}$, $\{u^k\}$, and $\{y^k\}$ be redefined as the subsequences indexed by $\{k_i\}$. For an arbitrary $v \in \mathbb{R}^d$, it holds that

$$f^\circ(y^k; v) \geq \langle u^k, v \rangle,$$

where $f^\circ(y^k; v)$ is the Clarke generalized directional derivative (Clarke, 1990, Proposition 2.1.2 (b)). Given that $f^\circ(w; v)$ is upper semicontinuous (Clarke, 1990, Proposition 2.1.1 (b)),

$$f^\circ(y; v) \geq \limsup_{k \rightarrow \infty} f^\circ(y^k; v) \geq \limsup_{k \rightarrow \infty} \langle u^k, v \rangle = \langle u, v \rangle.$$

As v was chosen arbitrarily, $u \in \partial g(y)$ (Clarke, 1990, Proposition 2.1.5 (a)).

Considering $\overline{B}_\epsilon^p(w)$ as a set-valued mapping in $w \in \mathbb{R}^d$, it is outer semicontinuous: For any $\gamma > 0$, $\overline{B}_\epsilon^p(B_\gamma^p(w)) = \{x : \exists y \in B_\gamma^p(w), \|x - y\|_p \leq \epsilon\} = \{x : \|x - w\|_p < \epsilon + \gamma\} = B_{\epsilon+\gamma}^p(w)$ (Rockafellar and Wets, 2009, Theorem 5.19). It follows that $y \in \overline{B}_\epsilon^p(w)$, and

$$u \in \partial g(y) \subseteq \hat{\partial}_\epsilon^p g(w),$$

proving that $\hat{\partial}_\epsilon^p g(w)$ is outer semicontinuous. It holds again by (Rockafellar and Wets, 2009, Theorem 5.19) that for any $\gamma > 0$, there exists a $\delta > 0$ such that

$$\hat{\partial}_\epsilon^p g(x) \subseteq \hat{\partial}_\epsilon^p g(w) + B_\gamma^p(w)$$

for all $x \in B_\delta^p(w)$. Taking the convex hulls of both sides,

$$\partial_\epsilon^p g(x) \subseteq \partial_\epsilon^p g(w) + B_\gamma^p(w)$$

(Schneider, 2014, Theorem 1.1.2) for all $x \in B_\delta^p(w)$, proving that $\partial_\epsilon^p g(w)$ is outer semicontinuous as well. \square

Proof. (Proposition 2): Consider any $w \in \mathbb{R}^d$ and any $\epsilon > 0$. The proof uses (Rockafellar and Wets, 2009, Proposition 5.49) and (Rockafellar and Wets, 2009, Inequality 4(13)).

For any $\alpha_k > 0$, the Pompeiu-Hausdorff distance (Rockafellar and Wets, 2009, Example 4.13) between $\hat{\partial}_{\alpha_k}^p g(w)$ and $\partial g(w)$ with respect to the chosen p -norm⁷ equals

$$\begin{aligned} & d_\infty^p(\hat{\partial}_{\alpha_k}^p g(w), \partial g(w)) \\ &= \inf\{\gamma \geq 0 : \hat{\partial}_{\alpha_k}^p g(w) \subseteq \partial g(w) + \overline{B}_\gamma^p(w), \partial g(w) \subseteq \hat{\partial}_{\alpha_k}^p g(w) + \overline{B}_\gamma^p(w)\} \\ &= \inf\{\gamma \geq 0 : \hat{\partial}_{\alpha_k}^p g(w) \subseteq \partial g(w) + \overline{B}_\gamma^p(w)\}. \end{aligned}$$

By the outer semicontinuity of $\partial g(w)$, there exists a $\delta > 0$, such that $\partial g(\overline{B}_\delta^p(w)) \subseteq \partial g(w) + \overline{B}_\epsilon^p(w)$. There exists a $K \in \mathbb{N}$ such that for all $j \geq K$, $\alpha_j \leq \delta$, implying that $\hat{\partial}_{\alpha_j}^p g(w) = \partial g(\overline{B}_{\alpha_j}^p(w)) \subseteq \partial g(w) + \overline{B}_\epsilon^p(w)$. Let j' be any $j \geq K$.

For any $k \in \mathbb{N}$, there exists a $\overline{K} \in \mathbb{N}$ such that for all $i \geq \overline{K}$, $\alpha_i \leq \frac{\alpha_k}{2}$, from which it holds that for $x \in \overline{B}_{\alpha_k}^p(w)$, $\hat{\partial}_{\alpha_i}^p g(x) \subseteq \hat{\partial}_{\alpha_k}^p g(w)$ for all $i \geq \overline{K}$, i.e. $\hat{\partial}_{\alpha_i}^p g(\overline{B}_{\alpha_k}^p(w)) \subseteq \hat{\partial}_{\alpha_k}^p g(w)$ for all $i \geq \overline{K}$.

In particular, there exists a $\overline{K} > j'$ such that for all $x \in \overline{B}_{\alpha_k}^p(w)$, for all $i \geq \overline{K}$, $\hat{\partial}_{\alpha_i}^p g(x) \subseteq \hat{\partial}_{\alpha_j}^p g(w) \subseteq \partial g(w) + \overline{B}_\epsilon^p(w)$, from which $d_\infty^p(\hat{\partial}_{\alpha_i}^p g(x), \partial g(w)) \leq \epsilon$. Given that $\partial g(w)$ and $\overline{B}_\epsilon^p(w)$ are convex sets, taking the convex hull of both sides, it also holds that for all $x \in \overline{B}_{\alpha_k}^p(w)$ and for all $i \geq \overline{K}$, $\partial_{\alpha_i}^p g(x) \subseteq \partial g(w) + \overline{B}_\epsilon^p(w)$, implying that $d_\infty^p(\partial_{\alpha_i}^p g(x), \partial g(w)) \leq \epsilon$ as well, proving that $\partial_{\alpha_k}^p g(w)$ and $\hat{\partial}_\epsilon^p g(w)$ converge continuously to $\partial g(w)$ for all $w \in \mathbb{R}^d$. \square

Proof. (Proposition 3): The function $f(w)$ is $\mathbb{E}[L_0]$ -Lipschitz continuous (Metel, 2022, Proposition 2). Let $\tilde{\nabla} f(w)$ be a Borel measurable function equal to the gradient of $f(w)$ almost everywhere it exists, see (Metel and Takeda, 2022, Example A.1) for a method of its construction. It holds that $\nabla f(w+u) \in \partial f(w+u)$ when $f(w+u)$ is differentiable (Clarke, 1990, Proposition 2.2.2), which is for almost all $u \in \overline{B}_{\frac{\alpha}{2}}^\infty$ by Rademacher's theorem. It follows that for almost all $u \in \overline{B}_{\frac{\alpha}{2}}^\infty$, $\tilde{\nabla} f(w+u) \in \partial_{\frac{\alpha}{2}}^\infty f(w)$, hence $\mathbb{E}[\tilde{\nabla} f(w+u)] \in \partial_{\frac{\alpha}{2}}^\infty f(w)$. The result follows given that $\nabla f_\alpha(w) = \mathbb{E}[\tilde{\nabla} f(w+u)]$ (Metel, 2022, Proposition 3). \square

9 Further Background on Finite-Precision Environments & Proofs of Section 3

9.1 Further Background on Finite-Precision Environments

Continuing from the definition of \mathbb{L}_N in Section 3, the subnormal floating-point numbers \mathbb{L}_S are the remaining small in magnitude non-zero numbers which do not use the full precision of \mathbb{L} , written as $y = \pm \beta^{e_{\min}} \times .0d_2 \dots d_t$. We do not need a signed 0 in this work, so let 0 be represented as $+\beta^{e_{\min}} \times .00(\dots)0$.

⁷This is done for simplicity, with the result holding using any norm on \mathbb{R}^d given their equivalence.

It follows that for any $y \in \mathbb{L}_N$, $\lambda_N \leq |y| \leq \beta^{e_{max}}(1 - \beta^{-t}) =: \Lambda^+$ and for any $y \in \mathbb{L}_S$, $\lambda = \beta^{e_{min}-t} \leq |y| \leq \lambda_N - \lambda$. In addition, it holds that $\Lambda^- = -\Lambda^+$.

For an \mathbb{I} with $\beta = 2$, the non-negative and negative numbers will have $e_r = 0$ and $e_r = 1$, respectively, and the range of representable numbers equals $[-2^{r-1}, 2^{r-1} - 2^{-t}]$. This can be generalized to arbitrary $\beta \in \mathbb{Z}_{>1}$.

Proposition 20. *The range of \mathbb{I} written in the form of (3) with base β using radix complement equals*

$$\left[-\left\lfloor \frac{\beta^{r+t}}{2} \right\rfloor \beta^{-t}, (\beta^{r+t} - \left\lfloor \frac{\beta^{r+t}}{2} \right\rfloor - 1) \beta^{-t}\right]. \quad (15)$$

Proof. The representable numbers are centered around 0, and when β is even, with an even number of representable numbers, β^{r+t} , the representable numbers are evenly assigned to negative and non-negative numbers, resulting in there being one more negative number, $[(\beta - 1)00\dots 0.00\dots 0]$, than there is positive numbers. When β is odd, β^{r+t} is odd, hence the representation is symmetric.

The equation (15) can be interpreted as there being $n = \lfloor \frac{\beta^{r+t}}{2} \rfloor$ negative numbers and $\beta^{r+t} - n$ non-negative numbers. With the difference between adjacent representable numbers equal to $\rho := \beta^{-t}$, the smallest number is then $-n\rho$ and the largest number is $(\beta^{r+t} - n - 1)\rho$.

When β is even, $\lfloor \frac{\beta^{r+t}}{2} \rfloor = \frac{\beta^{r+t}}{2}$, hence the negative and non-negative numbers have been evenly divided. When β is odd, let even $m := \beta^{r+t} - 1$. It follows that $n = \lfloor \frac{\beta^{r+t}}{2} \rfloor = \lfloor \frac{m+1}{2} \rfloor = \frac{m}{2}$ and $\beta^{r+t} - \lfloor \frac{\beta^{r+t}}{2} \rfloor - 1 = m + 1 - \frac{m}{2} - 1 = \frac{m}{2}$, hence the number of negative and positive numbers are equal. \square

For an \mathbb{I} , $\Lambda^- = -\lfloor \frac{\beta^{r+t}}{2} \rfloor \beta^{-t}$, $\Lambda^+ = (\beta^{r+t} - \lfloor \frac{\beta^{r+t}}{2} \rfloor - 1) \beta^{-t}$ and $\lambda = \beta^{-t}$. The following proposition proves that tie-breaking rules are unnecessary when using rounding to nearest in an odd base \mathbb{F} by considering a number of the form $y = 0.d_1d_2\dots d_t$ with $t \in \mathbb{Z}_{>0}$. This is without loss of generality, with more discussion after the proof of the result.

Proposition 21. *Consider a $y \in \mathbb{F}$ with an odd base β and $t \in \mathbb{Z}_{>0}$ of the form $y = 0.d_1d_2\dots d_t$. For any $q \in \mathbb{Z}_{\geq 0}$, it holds that $\underset{z \in \{d'_0, d'_1, d'_2, \dots, d'_q; 0 \leq d'_i \leq \beta-1 \forall i \in [q]_0\}}{\operatorname{argmin}} |y - z|$ is a singleton.*

Proof. The result is trivial when $q \geq t$, so we will assume that $q < t$. The argmin will not be a singleton when $d_q\beta^{-q} + d_{q+1}\beta^{-(q+1)} + \dots d_t\beta^{-t}$ is equidistant from $d_q\beta^{-q}$ and $(d_q + 1)\beta^{-q}$, i.e.

$$\begin{aligned} d_q\beta^{-q} + \dots + d_t\beta^{-t} - d_q\beta^{-q} &= (d_q + 1)\beta^{-q} - (d_q\beta^{-q} + \dots + d_t\beta^{-t}) \\ \Rightarrow d_{q+1}\beta^{-(q+1)} + \dots + d_t\beta^{-t} &= \beta^{-q} - (d_{q+1}\beta^{-(q+1)} + \dots + d_t\beta^{-t}) \\ \Rightarrow 2(d_{q+1}\beta^{-(q+1)} + \dots + d_t\beta^{-t}) &= \beta^{-q} \\ \Rightarrow 2(d_{q+1}\beta^{t-(q+1)} + \dots + d_t\beta^0) &= \beta^{t-q}, \end{aligned}$$

which is impossible given that the left-hand side is an even integer, whereas the right-hand side is odd. \square

When $\mathbb{F} = \mathbb{L}$, Proposition 21 is considering a number of the form $y = +\beta^0.d_1d_2\dots d_t$. Given that all \mathbb{L} are symmetric about 0, the result also holds for when $\pm = -$. The assumption that $e = 0$ is without loss of generality. If y gets rounded up to $y = 1.00\dots$, considering its true exponent e , y is rounded to $y = \beta^{e+1}0.100\dots$, with a possible overflow, see (IEEE Computer Society, 2019, Section 7.4), having no effect on the uniqueness of the rounding. If y gets rounded down, d_1 will not be decreased given that $q \in \mathbb{Z}_{>0}$ for any \mathbb{L} by definition, hence the true exponent e will be unchanged. For the case $\mathbb{F} = \mathbb{I}$, if in fact $t = 0$, i.e. $y \in \mathbb{Z}$, increasing t to a $q \in \mathbb{Z}_{>0}$ has no rounding effect. For a $y = [e_re_{r-1}(\dots)e_1.d_1d_2(\dots)d_t]$ with $r \in \mathbb{Z}_{\geq 0}$ and $t \in \mathbb{Z}_{>0}$, the uniqueness of rounding $y' = [0.d_1d_2(\dots)d_t]$ to $z' = [d'_0.d'_1d'_2(\dots)d'_q]$ implies the uniqueness of rounding y to $z = [e_re_{r-1}(\dots)e_1.0(\dots)0] + [0(\dots)d'_0.d'_1d'_2(\dots)d'_q]$, with again a possible overflow occurring, but with no effect on the uniqueness of the rounding operation.

9.2 Proofs of Section 3

Proof. (Proposition 4): For simplicity let $\widehat{\mathbb{L}} := \{y \in \mathbb{I}_{t,e_{min}}^{\beta,e_{max}} : \beta \in \mathbb{Z}_{>1}, t \in \mathbb{Z}_{>0}, \mathbb{Z} \ni e_{min} \leq e_{max} \in \mathbb{Z}\}$ and $\widehat{\mathbb{I}} := \{y \in \mathbb{I}_{r,t}^{\beta} : \beta \in \mathbb{Z}_{>1}, r \in \mathbb{Z}_{\geq 0}, t \in \mathbb{Z}_{\geq 0}, r + t \in \mathbb{Z}_{>0}\}$.

We first show that $\mathbb{Q} \subseteq \widehat{\mathbb{I}}$: For $y \in \mathbb{Q}$ let $|y|$ be representable as $|y| = \frac{a}{b}$ for $a \in \mathbb{Z}_{\geq 0}$ and $b \in \mathbb{Z}_{>0}$. Let $c, d \in \mathbb{Z}_{\geq 0}$ be the unique integers satisfying

$$a = cb + d \quad \text{and} \quad d < b.$$

It holds that $|y| \in \mathbb{I}_{r,1}^b$ if r satisfies, following Proposition 20,

$$\begin{aligned} (b^{r+1} - \lfloor \frac{b^{r+1}}{2} \rfloor - 1)b^{-1} &\geq \frac{cb + d}{b} \\ \Rightarrow \quad b^{r+1} - \lfloor \frac{b^{r+1}}{2} \rfloor - 1 &\geq cb + d, \end{aligned}$$

which is satisfied when

$$\begin{aligned} \frac{b^{r+1}}{2} - 1 &\geq cb + d \\ \Rightarrow \quad r &\geq \frac{\log(2(cb + d + 1))}{\log(b)} - 1. \end{aligned}$$

For $r^* \geq \frac{\log(2(cb + d + 1))}{\log(b)} - 1$, the radix complement of $-|y|$ is in $\mathbb{I}_{r^*,1}^b$ as well, hence $y \in \widehat{\mathbb{I}}$.

We now show that for a $y \in \widehat{\mathbb{I}}$ it holds that $y \in \mathbb{Q}$. From (3), its absolute value

$$|y| = \sum_{i=1}^r e_i \beta^{i-1} + \sum_{j=1}^t d_j \beta^{-j},$$

where each $e_i \beta^{i-1} \in \mathbb{Z}$ and each $d_j \beta^{-j} \in \mathbb{Q}$. It follows that $|y| \in \mathbb{Q}$ as a finite sum of rationals, from which it holds that $y \in \mathbb{Q}$ as well. Similarly for $y \in \widehat{\mathbb{L}}$, from (2),

$$|y| = \sum_{i=1}^t d_i \beta^{e-i}$$

is equal to a finite sum of rationals, hence $y \in \mathbb{Q}$. \square

Proof. (Proposition 5): For completeness we will give a proof that $\mathbb{E}[\delta] = 0$. Let $\omega := \lceil x \rceil_{\mathbb{F}} - \lfloor x \rfloor_{\mathbb{F}}$, noting that $\lceil x \rceil_{\mathbb{F}} - x = \omega - (x - \lfloor x \rfloor_{\mathbb{F}})$.

$$\begin{aligned} \mathbb{E}[\delta] &= (\lceil x \rceil_{\mathbb{F}} - x) \frac{x - \lfloor x \rfloor_{\mathbb{F}}}{\omega} + (\lfloor x \rfloor_{\mathbb{F}} - x) \left(1 - \frac{x - \lfloor x \rfloor_{\mathbb{F}}}{\omega}\right) \\ &= (\lceil x \rceil_{\mathbb{F}} - x) \frac{x - \lfloor x \rfloor_{\mathbb{F}}}{\omega} + (\lfloor x \rfloor_{\mathbb{F}} - x) \frac{\omega - (x - \lfloor x \rfloor_{\mathbb{F}})}{\omega} \\ &= (\lceil x \rceil_{\mathbb{F}} - x) \frac{x - \lfloor x \rfloor_{\mathbb{F}}}{\omega} + (\lfloor x \rfloor_{\mathbb{F}} - x) \frac{\lceil x \rceil_{\mathbb{F}} - x}{\omega} = 0. \end{aligned}$$

Letting $\kappa := x - \lfloor x \rfloor_{\mathbb{F}}$,

$$\begin{aligned} \text{Var}[\delta] &= \mathbb{E}[\delta^2] - \mathbb{E}[\delta]^2 \\ &= (\lceil x \rceil_{\mathbb{F}} - x)^2 \frac{x - \lfloor x \rfloor_{\mathbb{F}}}{\omega} + (\lfloor x \rfloor_{\mathbb{F}} - x)^2 \left(1 - \frac{x - \lfloor x \rfloor_{\mathbb{F}}}{\omega}\right) \\ &= (\omega - \kappa)^2 \frac{\kappa}{\omega} + \kappa^2 \frac{\omega - \kappa}{\omega} \\ &= \frac{\kappa}{\omega} (\omega^2 - 2\omega\kappa + \kappa^2 + \kappa\omega - \kappa^2) \\ &= \kappa\omega - \kappa^2 \\ &\leq \frac{\omega^2}{2} - \frac{\omega^2}{4} \\ &= \frac{(\lceil x \rceil_{\mathbb{F}} - \lfloor x \rfloor_{\mathbb{F}})^2}{4}, \end{aligned} \tag{16}$$

where the inequality holds given that $k = \frac{\omega}{2}$ maximizes the strongly concave function (16). From (3), $\lceil x \rceil_{\mathbb{I}} - \lfloor x \rfloor_{\mathbb{I}} \leq \beta^{-t}$, and from (2), $\lceil x \rceil_{\mathbb{L}} - \lfloor x \rfloor_{\mathbb{L}} \leq \beta^{(e-t)}$, where if $x > 0$, e is the exponent of $\lfloor x \rfloor_{\mathbb{F}}$, and if $x < 0$, e is the exponent of $\lceil x \rceil_{\mathbb{L}}$, which is the exponent of the representation of $\lfloor |x| \rfloor_{\mathbb{L}}$, see the image on (Higham, 2002, Page 38) for an intuition in $\beta = 2$. \square

Proof. (Proposition 6): We assume that all considered functions have a domain equal to \mathbb{R} . For any \mathbb{F} , the number of representable numbers, denoted as $|\mathbb{F}|$, is finite: for any \mathbb{L} , $|\mathbb{L}| = 1 + 2(e_{max} - e_{min} + 1)(\beta - 1)\beta^{t-1} + 2(\beta^{t-1} - 1)$, see the solution to (Higham, 2002, Problem 2.1), and for any \mathbb{I} , $|\mathbb{I}|$ equals β^{r+t} . For any \mathbb{F} , let the representable numbers be indexed from 1 to $|\mathbb{F}|$ in ascending order, i.e. $\mathbb{F} = \{y_{\mathbb{F}}^i\}_{i=1}^{|\mathbb{F}|}$ and $y_{\mathbb{F}}^i < y_{\mathbb{F}}^{i+1}$ for all $i \in [|\mathbb{F}| - 1]$.

Let $\mathcal{R}_{\mathbb{F}} := \{x \in \mathbb{R} : \Lambda^- \leq x \leq \Lambda^+\}$, which is the range of \mathbb{F} . We first verify the measurability of $\lfloor x \rfloor_{\mathbb{F}}$ and $\lceil x \rceil_{\mathbb{F}}$:

$$\lfloor x \rfloor_{\mathbb{F}} = \Lambda^- \mathbb{1}_{\{-\infty < x < \Lambda^-\}} + \sum_{i=1}^{|\mathbb{F}|-1} y_{\mathbb{F}}^i \mathbb{1}_{\{y_{\mathbb{F}}^i \leq x < y_{\mathbb{F}}^{i+1}\}} + \Lambda^+ \mathbb{1}_{\{\Lambda^+ \leq x < \infty\}}$$

and

$$\lceil x \rceil_{\mathbb{F}} = \Lambda^- \mathbb{1}_{\{-\infty < x \leq \Lambda^-\}} + \sum_{i=2}^{|\mathbb{F}|} y_{\mathbb{F}}^i \mathbb{1}_{\{y_{\mathbb{F}}^{i-1} < x \leq y_{\mathbb{F}}^i\}} + \Lambda^+ \mathbb{1}_{\{\Lambda^+ < x < \infty\}},$$

where all $x \notin \mathcal{R}_{\mathbb{F}}$ are set to whichever is closest between Λ^- and Λ^+ . Since both $\lfloor x \rfloor_{\mathbb{F}}$ and $\lceil x \rceil_{\mathbb{F}}$ are simple functions (Folland, 1999, Page 46), they are measurable. Similarly, rounding to nearest is also a simple function, hence measurable:

$$R(x) = \Lambda^- \mathbb{1}_{\{-\infty < x \lesssim \frac{\Lambda^- + y_{\mathbb{F}}^2}{2}\}} + \sum_{i=2}^{|\mathbb{F}|-1} y_{\mathbb{F}}^i \mathbb{1}_{\{\frac{y_{\mathbb{F}}^{i-1} + y_{\mathbb{F}}^i}{2} \lesssim x \lesssim \frac{y_{\mathbb{F}}^i + y_{\mathbb{F}}^{i+1}}{2}\}} + \Lambda^+ \mathbb{1}_{\{\frac{y_{\mathbb{F}}^{|\mathbb{F}|-1} + \Lambda^+}{2} \lesssim x < \infty\}},$$

where in each instance, $\lesssim = <$ or \leq , depending on the tie-breaking rule.

For stochastic rounding, for $u \in [0, 1]$, the function

$$R(x, u) = \lceil x \rceil_{\mathbb{F}} \mathbb{1}_{\{u(\lceil x \rceil_{\mathbb{F}} - \lfloor x \rfloor_{\mathbb{F}}) - (x - \lfloor x \rfloor_{\mathbb{F}}) \leq 0\}} + \lfloor x \rfloor_{\mathbb{F}} \mathbb{1}_{\{u(\lceil x \rceil_{\mathbb{F}} - \lfloor x \rfloor_{\mathbb{F}}) - (x - \lfloor x \rfloor_{\mathbb{F}}) > 0\}}$$

performs stochastic rounding of x when inputting a sample $u \sim U([0, 1])$: when $x \in \mathcal{R}_{\mathbb{F}}$ and $x \notin \mathbb{F}$, $R(x, u) = \lceil x \rceil_{\mathbb{F}}$ when $u \leq \frac{x - \lfloor x \rfloor_{\mathbb{F}}}{\lceil x \rceil_{\mathbb{F}} - \lfloor x \rfloor_{\mathbb{F}}}$ and $R(x, u) = \lfloor x \rfloor_{\mathbb{F}}$ when $u > \frac{x - \lfloor x \rfloor_{\mathbb{F}}}{\lceil x \rceil_{\mathbb{F}} - \lfloor x \rfloor_{\mathbb{F}}}$. When $x \in \mathbb{F}$ or $x \notin \mathcal{R}_{\mathbb{F}}$, $\lceil x \rceil_{\mathbb{F}} = \lfloor x \rfloor_{\mathbb{F}}$ and one of x , Λ^+ , or Λ^- is correctly returned. In addition, $R(x, u)$ is measurable over the product measurable space $(\mathbb{R} \times [0, 1], \mathcal{B}_{\mathbb{R}} \otimes \mathcal{B}_{[0,1]})$, given the measurability of $\lceil x \rceil_{\mathbb{F}}$ and $\lfloor x \rfloor_{\mathbb{F}}$. \square

10 Proofs of Section 5

Proof. (Proposition 8): Let $S := \{w^i, \xi^i\}_{i=1}^{\infty} \subset \mathbb{R}^{d+p}$ be the set of points where $\widehat{\nabla}F(w, \xi, b)$ approximates $\widetilde{\nabla}F(w, \xi)$, and let $V := \{b : b_j \in V_j \forall j \in [s]\}$. By assumption, $\widetilde{\nabla}F(w, \xi)$ is a Borel measurable function in \mathbb{R}^{d+p} . Define $\widehat{\nabla}F(w, \xi, b) := \widetilde{\nabla}F(w, \xi)$ for all $(w, \xi, b) \in S^c \times \mathbb{R}^s$. When $(w, \xi, b) \in S \times V^c$, define $\widehat{\nabla}F(w, \xi, b) := a$ for any $a \in \mathbb{R}^d$. For any $i \in [d]$ and $\hat{a} \in \mathbb{R}$, the set

$$\begin{aligned} & \{(w, \xi, b) \in \mathbb{R}^{d+p+s} : \widehat{\nabla}_i F(w, \xi, b) > \hat{a}\} \\ &= \{(w, \xi, b) \in S^c \times \mathbb{R}^s : \widetilde{\nabla}_i F(w, \xi) > \hat{a}\} \cup \{(w, \xi, b) \in S \times \mathbb{R}^s : \widehat{\nabla}_i F(w, \xi, b) > \hat{a}\}. \end{aligned}$$

Given that S is countable, S^c is measurable, and the set

$$\begin{aligned} & \{(w, \xi, b) \in S^c \times \mathbb{R}^s : \widetilde{\nabla}_i F(w, \xi) > \hat{a}\} \\ &= (\{(w, \xi) \in \mathbb{R}^{d+p} : \widetilde{\nabla}_i F(w, \xi) > \hat{a}\} \cap S^c) \times \mathbb{R}^d \end{aligned}$$

is measurable, given the measurability of $\widetilde{\nabla}_i F(w, \xi)$. The set

$$\begin{aligned} & \{(w, \xi, b) \in S \times \mathbb{R}^d : \widehat{\nabla}_i F(w, \xi, b) > \hat{a}\} \\ &= \{(w, \xi, b) \in S \times V : \widehat{\nabla}_i F(w, \xi, b) > \hat{a}\} \cup \{(w, \xi, b) \in S \times V^c : \widehat{\nabla}_i F(w, \xi, b) > \hat{a}\} \end{aligned}$$

is measurable given that the set $S \times V$ is countable in \mathbb{R}^{d+p+s} , and

$$\{(w, \xi, b) \in S \times V^c : \widehat{\nabla}_i F(w, \xi, b) > \hat{a}\} = \begin{cases} \emptyset & \text{if } \hat{a} \geq a \\ S \times V^c & \text{otherwise} \end{cases}$$

is measurable given that the Borel σ -algebra on \mathbb{R}^{d+p+s} , $\mathcal{B}_{\mathbb{R}^{d+p+s}} = \mathcal{B}_{\mathbb{R}^{d+p}} \otimes \mathcal{B}_{\mathbb{R}^s}$, hence $S \times V^c \in \mathcal{B}_{\mathbb{R}^{d+p+s}}$. Given that S^c is a set of full measure, $\widehat{\nabla} F(w, \xi, b) = \widetilde{\nabla} F(w, \xi)$ for almost all $(w, \xi) \in \mathbb{R}^{d+p}$. \square

Proof. (Proposition 10): Inequality (7) holds given that $\mathbb{E}[\widetilde{\nabla} F(w + u, \xi)] = \nabla f_\alpha(w)$ (Metel, 2022, Proposition 3) for all $w \in \mathbb{R}^d$. Inequalities (8) and (9) hold given that for almost all $(w, \xi) \in \mathbb{R}^{d+p}$, $\|\widetilde{\nabla} F(w, \xi)\|_2 \leq L_0(\xi)$ by the Lipschitz continuity of $F(w, \xi)$ (Metel and Takeda, 2022, Lemma 4.2). \square

Proof. (Proposition 11): Using the notation of the definition of batch normalization written in (Ioffe and Szegedy, 2015, Algorithm 1), consider a mini-batch of size 2, with $x_1 = 2$, $x_2 = 1$, $\epsilon = 0.25$, $\gamma = 1$, and $\beta = 0$. For an \mathbb{F} with $S := \{3, 2, 1, 1.5, 0.5, 0.25, -0.5\} \subseteq \mathbb{F}$ $y_i := x_i - \mu_\beta$ for $i \in [2]$, and $z := \sigma_\beta^2 + \epsilon$ can be computed exactly with $y_1 = z = 0.5$. The batch norm output for x_1 can be written as $\frac{y_1}{\sqrt{z} + \delta_1} + \delta_2$, where δ_1 is the stochastic rounding error from the square root operation and δ_2 is the subsequent error from the division. Computing the expected value of the output of batch normalization for x_1 using stochastic rounding,

$$\begin{aligned} & \mathbb{E}\left[\frac{y_1}{\sqrt{z} + \delta_1} + \delta_2\right] \\ &= \mathbb{E}\left[\mathbb{E}\left[\frac{y_1}{\sqrt{z} + \delta_1} + \delta_2 \mid y_1, z, \delta_1\right]\right] \\ &= \mathbb{E}\left[\frac{y_1}{\sqrt{z} + \delta_1} + \mathbb{E}[\delta_2 \mid y_1, z, \delta_1]\right] \\ &= \mathbb{E}\left[\frac{y_1}{\sqrt{z} + \delta_1}\right] \\ &= \frac{y_1}{\lceil \sqrt{z} \rceil_{\mathbb{F}} \lceil \sqrt{z} \rceil_{\mathbb{F}} - \lfloor \sqrt{z} \rfloor_{\mathbb{F}}} + \frac{y_1}{\lceil \sqrt{z} \rceil_{\mathbb{F}}} \left(1 - \frac{\sqrt{z} - \lfloor \sqrt{z} \rfloor_{\mathbb{F}}}{\lceil \sqrt{z} \rceil_{\mathbb{F}} - \lfloor \sqrt{z} \rfloor_{\mathbb{F}}}\right) \\ &= \frac{y_1}{\lceil \sqrt{z} \rceil_{\mathbb{F}} - \lfloor \sqrt{z} \rfloor_{\mathbb{F}}} \left(\frac{\sqrt{z} - \lfloor \sqrt{z} \rfloor_{\mathbb{F}}}{\lceil \sqrt{z} \rceil_{\mathbb{F}}} + \frac{\lceil \sqrt{z} \rceil_{\mathbb{F}} - \sqrt{z}}{\lfloor \sqrt{z} \rfloor_{\mathbb{F}}}\right). \end{aligned}$$

Assume that the expected error is 0:

$$\begin{aligned} & \frac{y_1}{\lceil \sqrt{z} \rceil_{\mathbb{F}} - \lfloor \sqrt{z} \rfloor_{\mathbb{F}}} \left(\frac{\sqrt{z} - \lfloor \sqrt{z} \rfloor_{\mathbb{F}}}{\lceil \sqrt{z} \rceil_{\mathbb{F}}} + \frac{\lceil \sqrt{z} \rceil_{\mathbb{F}} - \sqrt{z}}{\lfloor \sqrt{z} \rfloor_{\mathbb{F}}}\right) = \frac{y_1}{\sqrt{z}} \\ \Rightarrow \sqrt{z} \left(\frac{\sqrt{z} - \lfloor \sqrt{z} \rfloor_{\mathbb{F}}}{\lceil \sqrt{z} \rceil_{\mathbb{F}}} + \frac{\lceil \sqrt{z} \rceil_{\mathbb{F}} - \sqrt{z}}{\lfloor \sqrt{z} \rfloor_{\mathbb{F}}}\right) &= \lceil \sqrt{z} \rceil_{\mathbb{F}} - \lfloor \sqrt{z} \rfloor_{\mathbb{F}} \\ \Rightarrow \sqrt{z} \left(\frac{\lceil \sqrt{z} \rceil_{\mathbb{F}}}{\lceil \sqrt{z} \rceil_{\mathbb{F}}} - \frac{\lfloor \sqrt{z} \rfloor_{\mathbb{F}}}{\lfloor \sqrt{z} \rfloor_{\mathbb{F}}}\right) &= \lceil \sqrt{z} \rceil_{\mathbb{F}} - \lfloor \sqrt{z} \rfloor_{\mathbb{F}} + z \left(\frac{1}{\lceil \sqrt{z} \rceil_{\mathbb{F}}} - \frac{1}{\lfloor \sqrt{z} \rfloor_{\mathbb{F}}}\right). \end{aligned}$$

For any \mathbb{F} with $S \subseteq \mathbb{F}$ this is impossible to hold given that \sqrt{z} is irrational, and $\lceil \sqrt{z} \rceil_{\mathbb{F}}$ and $\lfloor \sqrt{z} \rfloor_{\mathbb{F}}$ are non-zero and rational from Proposition 4. It can never hold that $\lceil \sqrt{z} \rceil_{\mathbb{F}} = \lfloor \sqrt{z} \rfloor_{\mathbb{F}}$, hence the left-hand side is an irrational number, whereas the right-hand side is rational.

Batch normalization suffered from biased rounding error due to the division by \sqrt{z} in this example. In back propagation, this error will also occur as this operation is required when computing the gradient of batch normalization, see $\frac{\partial l}{\partial \mu_\beta}$ and $\frac{\partial l}{\partial x_i}$ in (Ioffe and Szegedy, 2015, Section 3). \square

Proof. (Proposition 12):

$$\begin{aligned}
& \mathbb{E}[\|\widehat{\nabla} \overline{F}^k(w^k)\|_2^2 | \mathcal{I}_k] \\
&= \mathbb{E}[\|\frac{1}{M} \sum_{i=1}^M \widehat{\nabla} F(w^k + \hat{u}^k, \xi^{k,i}, b^{k,i})\|_2^2 | \mathcal{I}_k] \\
&= \mathbb{E}[\sum_{j=1}^d (\frac{1}{M} \sum_{i=1}^M \widehat{\nabla} F_j(w^k + \hat{u}^k, \xi^{k,i}, b^{k,i}))^2 | \mathcal{I}_k] \\
&\leq \mathbb{E}[\sum_{j=1}^d \frac{1}{M} \sum_{i=1}^M \widehat{\nabla} F_j(w^k + \hat{u}^k, \xi^{k,i}, b^{k,i})^2 | \mathcal{I}_k] \\
&= \frac{1}{M} \sum_{i=1}^M \mathbb{E}[\|\widehat{\nabla} F(w^k + \hat{u}^k, \xi^{k,i}, b^{k,i})\|_2^2 | \mathcal{I}_k] \\
&\leq c_2 Q,
\end{aligned}$$

where the first inequality uses Jensen's inequality and the second uses (6). \square

Proof. (Proposition 13): We adapt the results of (Wilkinson, 1965, Page 4 & 5), which for the basic operations $\{+, -, \times, \div\}$ with rounding to nearest applied to $x, y \in \mathbb{I}_t^\beta$ gives absolute errors bounded by $\{0, 0, 0.5\beta^{-t}, 0.5\beta^{-t}\}$, respectively, assuming no overflow. With the adoption of stochastic rounding these errors are increased to $\{0, 0, \beta^{-t}, \beta^{-t}\}$, but with the benefit that the errors from the operations $\{\times, \div\}$ being unbiased.

Evaluating the left-hand side of (10),

$$\begin{aligned}
& w^k \ominus (\eta_k \otimes M) \otimes (\widehat{\nabla} F^{k,1}(w^k) \oplus \dots \oplus \widehat{\nabla} F^{k,M}(w^k)) \\
&= w^k - (\eta_k \otimes M) \otimes (\widehat{\nabla} F^{k,1}(w^k) \oplus \dots \oplus \widehat{\nabla} F^{k,M}(w^k)) \\
&= w^k - (\frac{\eta_k}{M} + \delta_0) \otimes (\widehat{\nabla} F^{k,1}(w^k) \oplus \dots \oplus \widehat{\nabla} F^{k,M}(w^k)) \\
&= w^k - (\frac{\eta_k}{M} + \delta_0) \otimes \sum_{i=1}^M \widehat{\nabla} F^{k,i}(w^k) \\
&= w^k - ((\frac{\eta_k}{M} + \delta_0) \sum_{i=1}^M \widehat{\nabla} F^{k,i}(w^k) + \delta^1) \\
&= w^k - \frac{\eta_k}{M} \sum_{i=1}^M \widehat{\nabla} F^{k,i}(w^k) - \delta_0 \sum_{i=1}^M \widehat{\nabla} F^{k,i}(w^k) - \delta^1,
\end{aligned}$$

where $\delta_0 \in \mathbb{R}$ is the error from the division, and $\delta^1 \in \mathbb{R}^d$ is the vector of errors from the multiplication. It holds that $e^k = -\delta_0 \sum_{i=1}^M \widehat{\nabla} F^{k,i}(w^k) - \delta^1$, and

$$\begin{aligned}
& \mathbb{E}[\|e^k\|_2^2 | \mathcal{I}_k] \\
&= \mathbb{E}[\|\delta_0 M \widehat{\nabla} \overline{F}^k(w^k) + \delta^1\|_2^2 | \mathcal{I}_k] \\
&= \mathbb{E}[\|\delta_0 M \widehat{\nabla} \overline{F}^k(w^k)\|_2^2 | \mathcal{I}_k] + 2\mathbb{E}[\langle \delta_0 M \widehat{\nabla} \overline{F}^k(w^k), \delta^1 \rangle | \mathcal{I}_k] + \mathbb{E}[\|\delta^1\|_2^2 | \mathcal{I}_k] \\
&= M^2 \mathbb{E}[\delta_0^2 \|\widehat{\nabla} \overline{F}^k(w^k)\|_2^2 | \mathcal{I}_k] + 2M \mathbb{E}[\langle \delta_0 \widehat{\nabla} \overline{F}^k(w^k), \delta^1 \rangle | \mathcal{I}_k] + \mathbb{E}[\|\delta^1\|_2^2 | \mathcal{I}_k]. \tag{17}
\end{aligned}$$

Focusing on $\mathbb{E}[\delta_0^2 \|\widehat{\nabla} \overline{F}^k(w^k)\|_2^2 | \mathcal{I}_k]$, given that δ_0^2 and $\|\widehat{\nabla} \overline{F}^k(w^k)\|_2^2$ are conditionally independent with respect to \mathcal{I}_k given that both η_k and w^k are \mathcal{I}_k -measurable,

$$\begin{aligned}
& \mathbb{E}[\delta_0^2 \|\widehat{\nabla} \overline{F}^k(w^k)\|_2^2 | \mathcal{I}_k] \\
&= \mathbb{E}[\delta_0^2 | \mathcal{I}_k] \mathbb{E}[\|\widehat{\nabla} \overline{F}^k(w^k)\|_2^2 | \mathcal{I}_k] \\
&\leq \frac{\beta^{-2t}}{4} c_2 Q,
\end{aligned}$$

using Propositions 5 and 12. Focusing now on $\mathbb{E}[\langle \delta_0 \widehat{\nabla} \overline{F}^k(w^k), \delta^1 \rangle | \mathcal{I}_k]$,

$$\begin{aligned}
& \mathbb{E}[\langle \delta_0 \widehat{\nabla} \overline{F}^k(w^k), \delta^1 \rangle | \mathcal{I}_k] \\
&= \mathbb{E}[\mathbb{E}[\langle \delta_0 \widehat{\nabla} \overline{F}^k(w^k), \delta^1 \rangle | \delta_0, \mathcal{G}_k, \mathcal{I}_k] | \mathcal{I}_k] \\
&= \mathbb{E}[\langle \delta_0 \widehat{\nabla} \overline{F}^k(w^k), \mathbb{E}[\delta^1 | \delta_0, \mathcal{G}_k, \mathcal{I}_k] \rangle | \mathcal{I}_k] \\
&= 0.
\end{aligned}$$

Continuing from (17),

$$\begin{aligned}
& \mathbb{E}[\|e^k\|_2^2 | \mathcal{I}_k] \\
&\leq M^2 \frac{\beta^{-2t}}{4} c_2 Q + \mathbb{E}[\|\delta^1\|_2^2 | \mathcal{I}_k] \\
&= M^2 \frac{\beta^{-2t}}{4} c_2 Q + \mathbb{E}\left[\sum_{i=1}^M (\delta_i^1)^2 | \mathcal{I}_k\right] \\
&= M^2 \frac{\beta^{-2t}}{4} c_2 Q + \sum_{i=1}^M \mathbb{E}[\mathbb{E}[(\delta_i^1)^2 | \delta_0, \mathcal{G}_k, \mathcal{I}_k] | \mathcal{I}_k] \\
&\leq M^2 \frac{\beta^{-2t}}{4} c_2 Q + \sum_{i=1}^M \frac{\beta^{-2t}}{4} \\
&= \frac{M}{4} (M c_2 Q + 1) \beta^{-2t} \\
&\leq \frac{M}{4} (M c_2 Q + 1) \eta^2,
\end{aligned}$$

where the last inequality holds since β^{-t} is the smallest positive element of \mathbb{I}_t^β .

□

Lemma 22. (Robbins and Siegmund, 1971, Theorem 1) For all $k \geq 1$, let z_k , θ_k , and ζ_k be non-negative \mathcal{I}_k -measurable random variables such that

$$\mathbb{E}[z_{k+1} | \mathcal{I}_k] \leq z_k + \theta_k - \zeta_k,$$

and assume that $\sum_{k=1}^{\infty} \theta_k < \infty$ almost surely. It holds that almost surely z_k converges to a random variable, $\lim_{k \rightarrow \infty} z_k = z_{\infty} < \infty$, and $\sum_{k=1}^{\infty} \zeta_k < \infty$.

Proof. (Theorem 14): This proof requires a Robbins-Siegmund inequality which is given directly above as Lemma 22. We begin the analysis assuming that the algorithm has been run sufficiently long such that $k \geq \bar{K}$ and Assumption 9 holds. By the L_1^α -smoothness of $f_\alpha(w)$ (Nesterov, 2004, Lemma 1.2.3),

$$\begin{aligned} f_{\alpha_k}(w^{k+1}) &\leq f_{\alpha_k}(w^k) + \langle \nabla f_{\alpha_k}(w^k), w^{k+1} - w^k \rangle + \frac{L_1^{\alpha_k}}{2} \|w^{k+1} - w^k\|_2^2 \\ &= f_{\alpha_k}(w^k) + \langle \nabla f_{\alpha_k}(w^k), -\eta_k \widehat{\nabla} \bar{F}^k(w^k) + e^k \rangle + \frac{L_1^{\alpha_k}}{2} \|w^{k+1} - w^k\|_2^2 \end{aligned} \quad (18)$$

$$\begin{aligned} \Rightarrow f_{\alpha_{k+1}}(w^{k+1}) &\leq f_{\alpha_k}(w^k) + f_{\alpha_{k+1}}(w^{k+1}) - f_{\alpha_k}(w^{k+1}) - \eta_k \langle \nabla f_{\alpha_k}(w^k), \widehat{\nabla} \bar{F}^k(w^k) \rangle \\ &\quad + \langle \nabla f_{\alpha_k}(w^k), e^k \rangle + \frac{L_1^{\alpha_k}}{2} \|w^{k+1} - w^k\|_2^2, \end{aligned} \quad (19)$$

Focusing on $f_{\alpha_{k+1}}(w^{k+1}) - f_{\alpha_k}(w^{k+1})$,

$$\begin{aligned} &f_{\alpha_{k+1}}(w^{k+1}) - f_{\alpha_k}(w^{k+1}) \\ &= f_{\alpha_{k+1}}(w^{k+1}) - \int_{-\alpha_k/2}^{\alpha_k/2} \int_{-\alpha_k/2}^{\alpha_k/2} \cdots \int_{-\alpha_k/2}^{\alpha_k/2} \frac{f(w^{k+1} + u)}{\alpha_k^d} du_1 du_2 \dots du_d \\ &= f_{\alpha_{k+1}}(w^{k+1}) - \int_{-\alpha_k/2}^{\alpha_k/2} \int_{-\alpha_k/2}^{\alpha_k/2} \cdots \int_{-\alpha_k/2}^{\alpha_k/2} \mathbb{1}_{\{u \in \mathbb{R}^d: \|u\|_\infty \leq \frac{\alpha_{k+1}}{2}\}} \frac{f(w^{k+1} + u)}{\alpha_k^d} du_1 du_2 \dots du_d \\ &\quad - \int_{-\alpha_k/2}^{\alpha_k/2} \int_{-\alpha_k/2}^{\alpha_k/2} \cdots \int_{-\alpha_k/2}^{\alpha_k/2} \mathbb{1}_{\{u \in \mathbb{R}^d: \|u\|_\infty > \frac{\alpha_{k+1}}{2}\}} \frac{f(w^{k+1} + u)}{\alpha_k^d} du_1 du_2 \dots du_d \\ &= f_{\alpha_{k+1}}(w^{k+1}) - f_{\alpha_{k+1}}(w^{k+1}) \frac{\alpha_{k+1}^d}{\alpha_k^d} \\ &\quad - \int_{-\alpha_k/2}^{\alpha_k/2} \int_{-\alpha_k/2}^{\alpha_k/2} \cdots \int_{-\alpha_k/2}^{\alpha_k/2} \mathbb{1}_{\{u \in \mathbb{R}^d: \|u\|_\infty > \frac{\alpha_{k+1}}{2}\}} \frac{f(w^{k+1} + u)}{\alpha_k^d} du_1 du_2 \dots du_d \\ &\leq f_{\alpha_{k+1}}(w^{k+1}) \left(1 - \frac{\alpha_{k+1}^d}{\alpha_k^d} \right), \end{aligned}$$

where we used the assumption that $\alpha_{k+1} \leq \alpha_k$ for the third equality, and that $\inf_{w \in \mathbb{R}^d} f(w) \geq 0$

for the inequality at the end. Plugging into (19),

$$\begin{aligned}
f_{\alpha_{k+1}}(w^{k+1}) &\leq f_{\alpha_k}(w^k) + f_{\alpha_{k+1}}(w^{k+1}) \left(1 - \frac{\alpha_{k+1}^d}{\alpha_k^d}\right) - \eta_k \langle \nabla f_{\alpha_k}(w^k), \widehat{\nabla} \overline{F}^k(w^k) \rangle \\
&\quad + \langle \nabla f_{\alpha_k}(w^k), e^k \rangle + \frac{L_1^{\alpha_k}}{2} \|w^{k+1} - w^k\|_2^2 \\
\Rightarrow \frac{\alpha_{k+1}^d}{\alpha_k^d} f_{\alpha_{k+1}}(w^{k+1}) &\leq f_{\alpha_k}(w^k) - \eta_k \langle \nabla f_{\alpha_k}(w^k), \widehat{\nabla} \overline{F}^k(w^k) \rangle \\
&\quad + \langle \nabla f_{\alpha_k}(w^k), e^k \rangle + \alpha_k^{-1} \sqrt{d} L_0 \| - \eta_k \widehat{\nabla} \overline{F}^k(w^k) + e^k \|_2^2 \\
\Rightarrow \alpha_{k+1}^d f_{\alpha_{k+1}}(w^{k+1}) &\leq \alpha_k^d f_{\alpha_k}(w^k) - \alpha_k^d \eta_k \langle \nabla f_{\alpha_k}(w^k), \widehat{\nabla} \overline{F}^k(w^k) \rangle + \alpha_k^d \langle \nabla f_{\alpha_k}(w^k), e^k \rangle \\
&\quad + \alpha_k^{d-1} \sqrt{d} L_0 (\eta_k^2 \| \widehat{\nabla} \overline{F}^k(w^k) \|_2^2 - 2\eta_k \langle \widehat{\nabla} \overline{F}^k(w^k), e^k \rangle + \|e^k\|_2^2). \tag{20}
\end{aligned}$$

Taking the conditional expectation of (20) with respect to \mathcal{I}_k ,

$$\begin{aligned}
\mathbb{E}[\alpha_{k+1}^d f_{\alpha_{k+1}}(w^{k+1}) | \mathcal{I}_k] &\leq \alpha_k^d f_{\alpha_k}(w^k) - \alpha_k^d \eta_k \langle \nabla f_{\alpha_k}(w^k), \mathbb{E}[\widehat{\nabla} \overline{F}^k(w^k) | \mathcal{I}_k] \rangle \\
&\quad + \alpha_k^d \langle \nabla f_{\alpha_k}(w^k), \mathbb{E}[e^k | \mathcal{I}_k] \rangle + \alpha_k^{d-1} \eta_k^2 \sqrt{d} L_0 \mathbb{E}[\| \widehat{\nabla} \overline{F}^k(w^k) \|_2^2 | \mathcal{I}_k] \\
&\quad - 2\alpha_k^{d-1} \eta_k \sqrt{d} L_0 \mathbb{E}[\langle \widehat{\nabla} \overline{F}^k(w^k), e^k \rangle | \mathcal{I}_k] + \alpha_k^{d-1} \sqrt{d} L_0 \mathbb{E}[\|e^k\|_2^2 | \mathcal{I}_k]. \tag{21}
\end{aligned}$$

Using inequality (5), 1. $-\alpha_k^d \eta_k \langle \nabla f_{\alpha_k}(w^k), \mathbb{E}[\widehat{\nabla} \overline{F}^k(w^k) | \mathcal{I}_k] \rangle \leq -\alpha_k^d \eta_k c_1 \| \nabla f_{\alpha_k}(w^k) \|_2^2$, 2. $\mathbb{E}[e^k | \mathcal{I}_k] = \mathbb{E}[\mathbb{E}[e^k | \mathcal{G}_k, \mathcal{I}_k] | \mathcal{I}_k] = 0$ by assumption, 3. $\mathbb{E}[\| \widehat{\nabla} \overline{F}^k(w^k) \|_2^2 | \mathcal{I}_k] \leq c_2 Q$ using Proposition 12,

4. $\mathbb{E}[\langle \widehat{\nabla} \overline{F}^k(w^k), e^k \rangle | \mathcal{I}_k] = \mathbb{E}[\mathbb{E}[\langle \widehat{\nabla} \overline{F}^k(w^k), e^k \rangle | \mathcal{G}_k, \mathcal{I}_k] | \mathcal{I}_k] = \mathbb{E}[\langle \widehat{\nabla} \overline{F}^k(w^k), \mathbb{E}[e^k | \mathcal{G}_k, \mathcal{I}_k] \rangle | \mathcal{I}_k] = 0$,

and 5. $\mathbb{E}[\|e^k\|_2^2 | \mathcal{I}_k] \leq c_3 \eta_k^2$ by assumption. Plugging these five updates into (21),

$$\begin{aligned}
\mathbb{E}[\alpha_{k+1}^d f_{\alpha_{k+1}}(w^{k+1}) | \mathcal{I}_k] &\leq \alpha_k^d f_{\alpha_k}(w^k) - \alpha_k^d \eta_k c_1 \| \nabla f_{\alpha_k}(w^k) \|_2^2 + \alpha_k^{d-1} \eta_k^2 \sqrt{d} L_0 c_2 Q + \alpha_k^{d-1} \eta_k^2 \sqrt{d} L_0 c_3 \\
&= \alpha_k^d f_{\alpha_k}(w^k) - \alpha_k^d \eta_k c_1 \| \nabla f_{\alpha_k}(w^k) \|_2^2 + \alpha_k^{d-1} \eta_k^2 \sqrt{d} L_0 (c_2 Q + c_3).
\end{aligned}$$

Lemma 22 can now be applied (redefining the index from $k = \overline{K}, \overline{K} + 1, \dots$ to $k = 1, 2, \dots$) with $z_k = \alpha_k^d f_{\alpha_k}(w^k)$, $\theta_k = \alpha_k^{d-1} \eta_k^2 \sqrt{d} L_0 (c_2 Q + c_3)$, and $\zeta_k = \alpha_k^d \eta_k c_1 \| \nabla f_{\alpha_k}(w^k) \|_2^2$, given that

$$\sum_{k=\overline{K}}^{\infty} \alpha_k^{d-1} \eta_k^2 \sqrt{d} L_0 (c_2 Q + c_3) \leq \sqrt{d} L_0 (c_2 Q + c_3) \sum_{k=1}^{\infty} \alpha_k^{d-1} \eta_k^2 < \infty$$

almost surely by assumption, proving that almost surely

$$\sum_{k=\overline{K}}^{\infty} \alpha_k^d \eta_k c_1 \| \nabla f_{\alpha_k}(w^k) \|_2^2 < \infty. \tag{22}$$

It follows that $\liminf_{k \rightarrow \infty} \| \nabla f_{\alpha_k}(w^k) \|_2 = 0$ almost surely, as for any $\epsilon > 0$ if there exists a $\overline{K}_2 \geq \overline{K}$ such that $\| \nabla f_{\alpha_k}(w^k) \|_2 \geq \epsilon$ for all $k \geq \overline{K}_2$,

$$\sum_{k=\overline{K}_2}^{\infty} \alpha_k^d \eta_k c_1 \| \nabla f_{\alpha_k}(w^k) \|_2^2 \geq c_1 \epsilon^2 \sum_{k=\overline{K}_2}^{\infty} \alpha_k^d \eta_k = \infty$$

almost surely, given that almost surely $\sum_{k=1}^{\infty} \alpha_k^d \eta_k = \infty$ by assumption and that $\sum_{k=1}^{\bar{K}_2-1} \alpha_k^d \eta_k$ is finite, contradicting (22). There then exists a subsequence of indices $\{k_i\}$ for which $\lim_{i \rightarrow \infty} \|\nabla f_{\alpha_{k_i}}(w^{k_i})\|_2 = \liminf_{k \rightarrow \infty} \|\nabla f_{\alpha_k}(w^k)\|_2 = 0$ almost surely. If w^* is an accumulation point of $\{w^{k_i}\}$, let $\{k_{i_j}\}$ be a subsequence of $\{k_i\}$ such that $\lim_{j \rightarrow \infty} w^{k_{i_j}} = w^*$. Given that $\partial_{0.5\alpha_{k_{i_j}}}^{\infty} f(w^{k_{i_j}})$ converges continuously to $\partial f(w^*)$ by Proposition 2, it holds that

$$\lim_{j \rightarrow \infty} \text{dist}(0, \partial_{0.5\alpha_{k_{i_j}}}^{\infty} f(w^{k_{i_j}})) = \text{dist}(0, \partial f(w^*))$$

(Rockafellar and Wets, 2009, Exercise 5.42 (b)). Since $\nabla f_{\alpha_{k_{i_j}}}(w^{k_{i_j}}) \in \partial_{0.5\alpha_{k_{i_j}}}^{\infty} f(w^{k_{i_j}})$ from Proposition 3,

$$\text{dist}(0, \partial f(w^*)) = \lim_{j \rightarrow \infty} \text{dist}(0, \partial_{0.5\alpha_{k_{i_j}}}^{\infty} f(w^{k_{i_j}})) \leq \lim_{j \rightarrow \infty} \|\nabla f_{\alpha_{k_{i_j}}}(w^{k_{i_j}})\|_2 = 0.$$

□

Proof. (Proposition 15): Setting $\alpha_k = \frac{1}{k^p}$ and $\hat{\eta}_k = \frac{1}{k^q}$, the sequences $\{\alpha_k\}$ and $\{\hat{\eta}_k\}$ satisfy the conditions of Theorem 14 if $0 < dp + q \leq 1$ and $(d-1)p + 2q > 1$, which holds when $0.5 < q < 1$ and $p = \frac{(1-q)}{d}$.

Setting $\eta_k = \psi_k \hat{\eta}_k$ for $k \geq 1$, $\sum_{k=1}^{\infty} \alpha_k^d \eta_k \geq \Psi^I \sum_{k=1}^{\infty} \alpha_k^d \hat{\eta}_k = \infty$ and $\sum_{k=1}^{\infty} \alpha_k^{d-1} \eta_k^2 \leq \Psi^S \sum_{k=1}^{\infty} \alpha_k^{d-1} \hat{\eta}_k^2 < \infty$ almost surely. □

Proof. (Corollary 16): Taking the conditional expectation with respect to \mathcal{I}_k of inequality (18) in the proof of Theorem 14, and simplifying the notation, letting $\eta := \frac{\tau}{\sqrt{K}}$,

$$\begin{aligned} \mathbb{E}[f_{\alpha}(w^{k+1})|\mathcal{I}_k] &\leq f_{\alpha}(w^k) + \langle \nabla f_{\alpha}(w^k), -\eta \mathbb{E}[\widehat{\nabla F}^k(w^k)|\mathcal{I}_k] + \mathbb{E}[e^k|\mathcal{I}_k] \rangle \\ &\quad + \frac{L_1^{\alpha_k}}{2} \mathbb{E}[\|w^{k+1} - w^k\|_2^2|\mathcal{I}_k] \\ &= f_{\alpha}(w^k) + \langle \nabla f_{\alpha}(w^k), -\eta \mathbb{E}[\widehat{\nabla F}^k(w^k)|\mathcal{I}_k] + \mathbb{E}[e^k|\mathcal{I}_k] \rangle \\ &\quad + \frac{\sqrt{d}L_0}{\alpha} \mathbb{E}[\eta^2 \|\widehat{\nabla F}^k(w^k)\|_2^2 - 2\eta \langle \widehat{\nabla F}^k(w^k), e^k \rangle + \|e^k\|_2^2|\mathcal{I}_k] \\ &\leq f_{\alpha}(w^k) - \eta c_1 \|\nabla f_{\alpha}(w^k)\|_2^2 + \frac{\sqrt{d}L_0\eta^2}{\alpha} (c_2Q + c_3), \end{aligned}$$

where the last inequality uses the five updates described below (21) in the proof of Theorem 14. Dividing by ηc_1 and rearranging,

$$\|\nabla f_{\alpha}(w^k)\|_2^2 \leq \frac{1}{\eta c_1} (f_{\alpha}(w^k) - \mathbb{E}[f_{\alpha}(w^{k+1})|\mathcal{I}_k]) + \frac{\sqrt{d}L_0\eta}{\alpha c_1} (c_2Q + c_3).$$

Taking the expectation, summing the inequalities over $k \in [K]$, and dividing by K ,

$$\frac{1}{K} \sum_{k=1}^K \mathbb{E}[\|\nabla f_{\alpha}(w^k)\|_2^2] \leq \frac{1}{\eta c_1 K} (f_{\alpha}(w^1) - \mathbb{E}[f_{\alpha}(w^{K+1})]) + \frac{\sqrt{d}L_0\eta}{\alpha c_1} (c_2Q + c_3).$$

Noting that $\mathbb{E}[\|\nabla f_\alpha(\hat{w})\|_2^2] = \frac{1}{K} \sum_{k=1}^K \mathbb{E}[\|\nabla f_\alpha(w^k)\|_2^2]$, $\mathbb{E}[\text{dist}(0, \partial_{\frac{\alpha}{2}}^\infty f(\hat{w}))^2] \leq \mathbb{E}[\|\nabla f_\alpha(\hat{w})\|_2^2]$ from Proposition 3, and that $\mathbb{E}[f_\alpha(w^{K+1})] \geq 0$ by assumption, and plugging in $\eta = \frac{\tau}{\sqrt{K}}$,

$$\mathbb{E}[\text{dist}(0, \partial_{\frac{\alpha}{2}}^\infty f(\hat{w}))^2] \leq \frac{f_\alpha(w^1)}{\tau c_1 \sqrt{K}} + \frac{\sqrt{d} L_0 \tau}{\alpha c_1 \sqrt{K}} (c_2 Q + c_3).$$

□

Lemma 23. *Let $R_t(\cdot)$ perform rounding to nearest into \mathbb{F}_t^d , and let $\frac{\alpha}{2} \in \mathbb{F}_t$ for an $\alpha > 0$. For any $y \in \overline{B}_{\frac{\alpha}{2}}^\infty \cap \mathbb{F}_t^d$, it holds that*

$$\overline{B}_{\frac{\alpha}{2}}^\infty \cap R_t^{-1}(y) \subseteq R_t^{-1}(y) \subseteq [y - \frac{\beta^{e-t}}{2}, y + \frac{\beta^{e-t}}{2}]^d \quad (23)$$

and $m(R_t^{-1}(y)) \geq m(\overline{B}_{\frac{\alpha}{2}}^\infty \cap R_t^{-1}(y)) \geq (\frac{\beta^{e-t-1}}{2})^d$, where $e = 0$ for $\mathbb{F} = \mathbb{I}$.

Proof. The distance from a point $y \in \mathbb{L}_t$, $y \notin \{\Lambda^-, \Lambda^+\}$ to the closest larger in magnitude element in \mathbb{L}_t equals β^{e-t} . The distance to the closest smaller in magnitude element for any $y \in \mathbb{L}_t$ equals β^{e-t-1} when $d_1 = 1$, $d_i = 0 \forall i > 1$, and $|y| \neq \lambda_N$, and β^{e-t} otherwise. When $\mathbb{F} = \mathbb{I}$, all points are β^{-t} apart. As $R_t(\cdot)$ rounds to nearest, it holds that $R_t^{-1}(y) \subseteq [y - \frac{\beta^{e-t}}{2}, y + \frac{\beta^{e-t}}{2}]$. When $y \in \{\Lambda^+, \Lambda^-\}$ this bound also holds as $R_t^{-1}(y) \subseteq S$ for an $S \in \{[y - \frac{\beta^{e-t}}{2}, y], [y, y + \frac{\beta^{e-t}}{2}]\}$. Expanding this bound up to d dimensions results in (23).

From the previous paragraph, the lower bound in one dimension for $y \in \mathbb{F}_t$, $m([- \frac{\alpha}{2}, \frac{\alpha}{2}] \cap R_t^{-1}(y)) \geq \frac{\beta^{e-t-1}}{2}$, is attained when considering $\mathbb{F} = \mathbb{L}$, $y = \frac{\alpha}{2}$, $d_1 = 1$, $d_i = 0 \forall i > 1$, and $|y| \neq \lambda_N$, as then $(y - \frac{\beta^{e-t-1}}{2}, y] \subseteq [- \frac{\alpha}{2}, \frac{\alpha}{2}] \cap R_t^{-1}(y)$. This lower bound is smaller than when considering $\mathbb{F} = \mathbb{I}$, where a lower bound on the inverse image of any $y \in [- \frac{\alpha}{2}, \frac{\alpha}{2}] \cap \mathbb{L}_t$ can be determined by considering $y \in \{- \frac{\alpha}{2}, \frac{\alpha}{2}\}$, with $S \subseteq [- \frac{\alpha}{2}, \frac{\alpha}{2}] \cap R_t^{-1}(y)$ for an $S \in \{(y - \frac{\beta^{-t}}{2}, y], [y, y + \frac{\beta^{-t}}{2}]\}$. The lower-bound in d -dimensions follows directly. □

Lemma 24. *Consider the counting measure on the countable set $\{y^k\}_{k=1}^\infty$. For any measurable set $S \in \mathbb{R}^d$ for which $m(S) = 0$, it holds that*

$$\begin{aligned} & \int_{w \in \mathbb{R}^d} \sum_{k=1}^\infty \mathbb{1}_{\{w+y^k \in S\}} dw \\ &= \sum_{k=1}^\infty \int_{w \in \mathbb{R}^d} \mathbb{1}_{\{w \in S - y^k\}} dw \\ &= \sum_{k=1}^\infty 0 = 0, \end{aligned}$$

where $S - y^k := \{s - y^k : s \in S\}$. The first equality uses Tonelli's theorem, given that $\mathbb{1}_{\{w+y^k \in S\}}$ is a non-negative measurable function and both measures are σ -finite.

Proof. (Theorem 18): This proof requires Lemmas 23 and 24 which are given directly above this proof. The first lemma is about the inverse image of $R_t(\cdot)$, and the second lemma states that if a property holds for almost all $w \in \mathbb{R}^d$, for a countable set $\{y^k\}_{k=1}^\infty$, it also holds for $\hat{w} := w + y^k \in \mathbb{R}^d$, for almost all $w \in \mathbb{R}^d$ and all $y^k \in \{y^k\}_{k=1}^\infty$. Following the assumptions of the theorem, for any $w \in \mathbb{R}^d$,

$$\begin{aligned} & \langle \mathbb{E}[\widehat{\nabla}F(w + R_{t_j}(u), \xi, b)], \nabla f_\alpha(w) \rangle \\ &= \langle \mathbb{E}[\widehat{\nabla}F(w + R_{t_j}(u), \xi, b)] - \mathbb{E}[\widehat{\nabla}F(w + u, \xi, b)] + \mathbb{E}[\widehat{\nabla}F(w + u, \xi, b)], \nabla f_\alpha(w) \rangle \\ &\geq \langle \mathbb{E}[\widehat{\nabla}F(w + R_{t_j}(u), \xi, b) - \widehat{\nabla}F(w + u, \xi, b)], \nabla f_\alpha(w) \rangle + c_1 \|\nabla f_\alpha(w)\|_2^2. \end{aligned} \quad (24)$$

Focusing on $\mathbb{E}[\widehat{\nabla}F(w + R_{t_j}(u), \xi, b) - \widehat{\nabla}F(w + u, \xi, b)]$,

$$\begin{aligned} & \mathbb{E}[\widehat{\nabla}F(w + R_{t_j}(u), \xi, b) - \widehat{\nabla}F(w + u, \xi, b)] \\ &= \sum_{k=1}^{|\hat{u}_{t_j}|} \mathbb{E}[\widehat{\nabla}F(w + \hat{u}_{t_j}^k, \xi, b) - \widehat{\nabla}F(w + u, \xi, b) | u \in R_{t_j}^{-1}(\hat{u}_{t_j}^k)] \mathbb{P}[R_{t_j}(u) = \hat{u}_{t_j}^k], \end{aligned}$$

using the law of total expectation, where $|\hat{u}_{t_j}|$ equals the number of elements in the image of \hat{u}_{t_j} . Continuing,

$$\begin{aligned} & \sum_{k=1}^{|\hat{u}_{t_j}|} \mathbb{E}[\widehat{\nabla}F(w + \hat{u}_{t_j}^k, \xi, b) - \widehat{\nabla}F(w + u, \xi, b) | u \in R_{t_j}^{-1}(\hat{u}_{t_j}^k)] \mathbb{P}[R_{t_j}(u) = \hat{u}_{t_j}^k] \\ &= \sum_{k=1}^{|\hat{u}_{t_j}|} \frac{m(\overline{B}_{\frac{\alpha}{2}}^\infty)}{m(\overline{B}_{\frac{\alpha}{2}}^\infty \cap R_{t_j}^{-1}(\hat{u}_{t_j}^k))} \mathbb{E}[(\widehat{\nabla}F(w + \hat{u}_{t_j}^k, \xi, b) - \widehat{\nabla}F(w + u, \xi, b)) \mathbb{1}_{u \in R_{t_j}^{-1}(\hat{u}_{t_j}^k)}] \mathbb{P}[R_{t_j}(u) = \hat{u}_{t_j}^k] \\ &= \sum_{k=1}^{|\hat{u}_{t_j}|} \frac{1}{m(\overline{B}_{\frac{\alpha}{2}}^\infty \cap R_{t_j}^{-1}(\hat{u}_{t_j}^k))} \int_{\overline{B}_{\frac{\alpha}{2}}^\infty \cap R_{t_j}^{-1}(\hat{u}_{t_j}^k)} \mathbb{E}_{\xi, b}[\widehat{\nabla}F(w + \hat{u}_{t_j}^k, \xi, b) - \widehat{\nabla}F(w + u, \xi, b)] du \mathbb{P}[R_{t_j}(u) = \hat{u}_{t_j}^k], \end{aligned} \quad (25)$$

for almost all $w \in \mathbb{R}^d$, using the fact that

$$\mathbb{P}[R_{t_j}(u) = \hat{u}_{t_j}^k] = \frac{m(\overline{B}_{\frac{\alpha}{2}}^\infty \cap R_{t_j}^{-1}(\hat{u}_{t_j}^k))}{m(\overline{B}_{\frac{\alpha}{2}}^\infty)}$$

for the first equality. The second equality holds using Fubini's theorem: for $i \in [d]$,

$$\begin{aligned} & \mathbb{E}[|\widehat{\nabla}_i F(w + \hat{u}_{t_j}^k, \xi, b) - \widehat{\nabla}_i F(w + u, \xi, b)| \mathbb{1}_{u \in R_{t_j}^{-1}(\hat{u}_{t_j}^k)}] \\ &\leq \mathbb{E}[|\widehat{\nabla}_i F(w + \hat{u}_{t_j}^k, \xi, b)| + |\widehat{\nabla}_i F(w + u, \xi, b)|] \\ &\leq \mathbb{E}[|\widehat{\nabla}F(w + \hat{u}_{t_j}^k, \xi, b)|_2 + |\widehat{\nabla}F(w + u, \xi, b)|_2] \\ &\leq \sqrt{c_2 Q} + \mathbb{E}[|\widehat{\nabla}F(w + u, \xi, b)|_2] \\ &\leq 2\sqrt{c_2 Q} \end{aligned} \quad (26)$$

for almost all $w \in \mathbb{R}^d$, where the second last inequality holds for almost all $w \in \mathbb{R}^d$ and the last inequality holds for all $w \in \mathbb{R}^d$ using (12) and Jensen's inequality, hence $(\widehat{\nabla}_i F(w + \hat{u}_{t_j}^k, \xi, b) - \widehat{\nabla}_i F(w + u, \xi, b)) \mathbb{1}_{u \in R_{t_j}^{-1}(\hat{u}_{t_j}^k)} \in L^1(P_u \times P_\xi \times P_b) = L^1(P_u \times (P_\xi \times P_b))$, for almost all $w \in \mathbb{R}^d$, where here P_X denotes the probability measure induced by a random variable X , with the associativity of the product of measures holding given that they are σ -finite (Folland, 1999, Section 2.5, Exercise 45).

Continuing from (25), we want to extend the sum to include all elements of $\hat{u}_\infty := \{y \in \{\hat{u}_{t_j}^k\} : j \geq 1\}$, which is countable from Proposition 4. To make things concrete we can index the elements of \hat{u}_∞ as follows: the elements of the 1-dimensional $\hat{u}_{\infty,1} := \{y_1 : y \in \{\hat{u}_{t_j}^k\}, j \geq 1\}$, considering the first element of each $y \in \{\hat{u}_{t_j}^k\}$, can be indexed by starting with $j = 1$ and assigning $\hat{u}_{\infty,1}^1 = 0$, $\hat{u}_{\infty,1}^2 = \min\{y_1 : y \in \{\hat{u}_{t_1}^k\}, y_1 > 0\}$, $\hat{u}_{\infty,1}^3 = \max\{y_1 : y \in \{\hat{u}_{t_1}^k\}, y_1 < 0\}$, and so on alternating between the next smallest positive and next biggest negative element of $\{y_1 : y \in \{\hat{u}_{t_1}^k\}\}$. When $\{y_1 : y \in \{\hat{u}_{t_1}^k\}\}$ is fully indexed, we add $\{y_1 : y \in \{\hat{u}_{t_2}^k\}, \exists i \in [2]_{t_1+1}, d_i \neq 0, \}$, which are the elements $\{y_1 : y \in \{\hat{u}_{t_2}^k\}, y_1 \notin \{y'_1 : y' \in \{\hat{u}_{t_1}^k\}\}\}$ in a similar manner, alternating between the smallest positive element and the largest negative element not yet indexed in $\{y_1 : y \in \{\hat{u}_{t_2}^k\}\}$, with this process continuing for all $j \geq 3$. The elements of $\hat{u}_{\infty,2} := \hat{u}_{\infty,1} \times \hat{u}_{\infty,1}$ can be indexed using Cantor's method of enumeration, such as commonly used for enumerating the rational numbers, and repeating this $d - 2$ times, finishing with $\hat{u}_\infty = \hat{u}_{\infty,d-1} \times \hat{u}_{\infty,1}$.

For a $j \geq 1$ and an element $\hat{u}^k \in \hat{u}_\infty$, if $\hat{u}^k \notin \{\hat{u}_{t_j}^{k'}\}$, $\frac{1}{m(\overline{B}_{\frac{\alpha}{2}} \cap R_{t_j}^{-1}(\hat{u}^k))} = \infty$, $\int_{\overline{B}_{\frac{\alpha}{2}} \cap R_{t_j}^{-1}(\hat{u}^k)} \mathbb{E}_{\xi,b}[\widehat{\nabla} F(w + \hat{u}_{t_j}^k, \xi, b) - \widehat{\nabla} F(w + u, \xi, b)] du = 0$, and $\mathbb{P}[R_{t_j}(u) = \hat{u}^k] = 0$. To avoid the consideration of $\infty \cdot 0$, let $j_k = \min\{j \geq 1 : \hat{u}^k \in \mathbb{F}_{t_j}^d\}$, or equivalently $j_k = \min\{j \geq 1 : \hat{u}^k \in \{\hat{u}_{t_j}^{k'}\}\}$. The equation (25) can now be written equivalently as

$$\sum_{k=1}^{\infty} \frac{\mathbb{P}[R_{t_{j_k}}(u) = \hat{u}^k]}{m(\overline{B}_{\frac{\alpha}{2}} \cap R_{t_{\max\{j,j_k\}}^{-1}}(\hat{u}^k))} \int_{\overline{B}_{\frac{\alpha}{2}} \cap R_{t_{\max\{j,j_k\}}^{-1}}(\hat{u}^k)} \mathbb{E}_{\xi,b}[\widehat{\nabla} F(w + \hat{u}^k, \xi, b) - \widehat{\nabla} F(w + u, \xi, b)] du, \quad (27)$$

given that still $\mathbb{P}[R_{t_j}(u) = \hat{u}^k] = 0$ when $\hat{u}^k \notin \{\hat{u}_{t_j}^{k'}\}$. Similar to computing (26), for any $w \in \mathbb{R}^d$, $i \in [d]$, and bounded measurable set $K \subset \mathbb{R}^d$,

$$\begin{aligned} & \int_{u \in K} |\mathbb{E}_{\xi,b}[\widehat{\nabla} F_i(w + u, \xi, b)]| du \\ & \leq \int_{u \in K} \|\mathbb{E}_{\xi,b}[\widehat{\nabla} F(w + u, \xi, b)]\|_2 du \\ & \leq \int_{u \in K} \sqrt{c_2 Q} du = m(K) \sqrt{c_2 Q} < \infty, \end{aligned} \quad (28)$$

given that $\mathbb{E}_{\xi,b}[\|\widehat{\nabla} F(w + u, \xi, b)\|_2^2] \leq c_2 Q$ for almost all $u \in K$, hence the functions $\mathbb{E}_{\xi,b}[\widehat{\nabla} F_i(w + u, \xi, b)]$ are locally integrable in $u \in \mathbb{R}^d$.

Using the Lebesgue differentiation theorem, by the local integrability of $\mathbb{E}[\widehat{\nabla} F_i(w + u, \xi, b)]$

(28), for almost all $w \in \mathbb{R}^d$, it holds that

$$\lim_{j \rightarrow \infty} \frac{1}{m(\overline{B}_{\frac{\alpha}{2}}^\infty \cap R_{t_{\max\{j, j_k\}}^{-1}}(\hat{u}^k))} \int_{\overline{B}_{\frac{\alpha}{2}}^\infty \cap R_{t_{\max\{j, j_k\}}^{-1}}(\hat{u}^k)} \mathbb{E}_{\xi, b}[\widehat{\nabla}F(w + \hat{u}^k, \xi, b) - \widehat{\nabla}F(w + u, \xi, b)] du = 0, \quad (29)$$

for all $\hat{u}^k \in \hat{u}^\infty$ using Lemma 24. In particular, we verify that the requirements of (Folland, 1999, Theorem 3.21) hold: for any $k \in \mathbb{N}$, from Lemma 23,

$$\overline{B}_{\frac{\alpha}{2}}^\infty \cap R_{t_{\max\{j, j_k\}}^{-1}}(\hat{u}^k) \subseteq [\hat{u}^k - \frac{\beta^{e-t_{\max\{j, j_k\}}}}{2}, \hat{u}^k + \frac{\beta^{e-t_{\max\{j, j_k\}}}}{2}]^d \subseteq \overline{B}_\rho^2(\hat{u}^k)$$

where $\rho = \sqrt{d} \frac{\beta^{e-t_{\max\{j, j_k\}}}}{2}$ and $m(\overline{B}_\rho^2(\hat{u}^k)) = \frac{(\sqrt{\pi}\rho)^d}{\Gamma(\frac{d}{2}+1)}$. The measure $m(\overline{B}_{\frac{\alpha}{2}}^\infty \cap R_{t_{\max\{j, j_k\}}^{-1}}(\hat{u}^k)) \geq (\frac{\beta^{e-t_{\max\{j, j_k\}}}}{2})^d$, hence

$$\begin{aligned} \frac{m(\overline{B}_{\frac{\alpha}{2}}^\infty \cap R_{t_{\max\{j, j_k\}}^{-1}}(\hat{u}^k))}{m(\overline{B}_\rho^2(\hat{u}^k))} &\geq \left(\frac{\beta^{e-t_{\max\{j, j_k\}}-1}}{2\sqrt{\pi}\rho} \right)^d \Gamma(\frac{d}{2} + 1) \\ &= \left(\frac{\beta^{e-t_{\max\{j, j_k\}}-1}}{2\sqrt{\pi}\sqrt{d} \frac{\beta^{e-t_{\max\{j, j_k\}}}}{2}} \right)^d \Gamma(\frac{d}{2} + 1) \\ &= \frac{\Gamma(\frac{d}{2} + 1)}{(\beta\sqrt{\pi d})^d}. \end{aligned} \quad (30)$$

The sets $\overline{B}_{\frac{\alpha}{2}}^\infty \cap R_{t_{\max\{j, j_k\}}^{-1}}(\hat{u}^k)$ are said to *shrink nicely*, given that (30) is a constant. A family of sets $\{E_\rho(\hat{u}^k)\}_{\rho>0}$ can be considered, which all satisfy

$$E_\rho(\hat{u}^k) \subseteq \overline{B}_\rho^2(\hat{u}^k)$$

and

$$\frac{m(E_\rho(\hat{u}^k))}{m(\overline{B}_\rho^2(\hat{u}^k))} \geq \frac{\Gamma(\frac{d}{2} + 1)}{(\beta\sqrt{\pi d})^d}.$$

From (Folland, 1999, Theorem 3.21), it holds that

$$\lim_{\rho \rightarrow 0} \frac{1}{m(E_\rho(\hat{u}^k))} \int_{E_\rho(\hat{u}^k)} \mathbb{E}_{\xi, b}[\widehat{\nabla}F(w + \hat{u}^k, \xi, b) - \widehat{\nabla}F(w + u, \xi, b)] du = 0 \quad (31)$$

for almost all $w \in \mathbb{R}^d$ and all $\hat{u}^k \in \hat{u}^\infty$ using Lemma 24: for a fixed $\hat{w} \in \mathbb{R}^d$, (31) holds for all values of \hat{u}^k (as an element of \mathbb{R}^d) outside of a set \hat{S} of Lebesgue measure 0 (Folland, 1999, Theorem 3.20). It follows that (31) holds when $w + \hat{u}^k \notin S := \{\hat{w} + s \in \mathbb{R}^d : s \in \hat{S}\}$. From Lemma 24 for almost all $w \in \mathbb{R}^d$, $w \notin \cup_{\hat{u}^k \in \hat{u}^\infty} (S - \hat{u}^k)$.

Considering values of ρ indexed by $j \geq 1$ such that $\rho_j = \sqrt{d} \frac{\beta^{e-t_{\max\{j, j_k\}}}}{2}$, and setting $E_{\rho_j}(\hat{u}^k) = \overline{B}_{\frac{\alpha}{2}}^\infty \cap R_{t_{\max\{j, j_k\}}}^{-1}(\hat{u}^k)$, it follows from (31), taking the limit over the sequence $j \geq 1$ that (29) holds for almost all $w \in \mathbb{R}^d$ and all $\hat{u}^k \in \hat{u}^\infty$.

In addition, for all $k \geq 1$,

$$\begin{aligned}
& \mathbb{P}[R_{t_j}(u) = \hat{u}^k] \\
& \leq \mathbb{P}[u \in [\hat{u}^k - \frac{\beta^{e-t_j}}{2}, \hat{u}^k + \frac{\beta^{e-t_j}}{2}]^d] \\
& = \frac{1}{m(\overline{B}_{\frac{\alpha}{2}}^\infty)} \int_{\max(\hat{u}^k - \frac{\beta^{e-t_j}}{2}, -\frac{\alpha}{2})}^{\min(\hat{u}^k + \frac{\beta^{e-t_j}}{2}, \frac{\alpha}{2})} \cdots \int_{\max(\hat{u}^k - \frac{\beta^{e-t_j}}{2}, -\frac{\alpha}{2})}^{\min(\hat{u}^k + \frac{\beta^{e-t_j}}{2}, \frac{\alpha}{2})} du_1 \dots du_d \\
& \leq \frac{1}{m(\overline{B}_{\frac{\alpha}{2}}^\infty)} \int_{\hat{u}^k - \frac{\beta^{e-t_j}}{2}}^{\hat{u}^k + \frac{\beta^{e-t_j}}{2}} \cdots \int_{\hat{u}^k - \frac{\beta^{e-t_j}}{2}}^{\hat{u}^k + \frac{\beta^{e-t_j}}{2}} du_1 \dots du_d \\
& = \frac{\beta^{(e-t_j)d}}{m(\overline{B}_{\frac{\alpha}{2}}^\infty)},
\end{aligned}$$

hence $\lim_{j \rightarrow \infty} \mathbb{P}[R_{t_j}(u) = \hat{u}^k] = 0$. Combining this with (29), it follows that for almost all $w \in \mathbb{R}^d$ and all $\hat{u}^k \in \hat{u}^\infty$,

$$\lim_{j \rightarrow \infty} \frac{\mathbb{P}[R_{t_j}(u) = \hat{u}^k]}{m(\overline{B}_{\frac{\alpha}{2}}^\infty \cap R_{t_{\max\{j, j_k\}}}^{-1}(\hat{u}^k))} \int_{\overline{B}_{\frac{\alpha}{2}}^\infty \cap R_{t_{\max\{j, j_k\}}}^{-1}(\hat{u}^k)} \mathbb{E}_{\xi, b}[\widehat{\nabla} F(w + \hat{u}^k, \xi, b) - \widehat{\nabla} F(w + u, \xi, b)] du = 0. \quad (32)$$

In addition, for almost all $w \in \mathbb{R}^d$, all $\hat{u}^k \in \hat{u}^\infty$, and any $i \in [d]$,

$$\begin{aligned}
& \left| \frac{\mathbb{P}[R_{t_j}(u) = \hat{u}^k]}{m(\overline{B}_{\frac{\alpha}{2}}^\infty \cap R_{t_{\max\{j, j_k\}}}^{-1}(\hat{u}^k))} \int_{\overline{B}_{\frac{\alpha}{2}}^\infty \cap R_{t_{\max\{j, j_k\}}}^{-1}(\hat{u}^k)} \mathbb{E}_{\xi, b}[\widehat{\nabla} F_i(w + \hat{u}^k, \xi, b) - \widehat{\nabla} F_i(w + u, \xi, b)] du \right| \\
& \leq \frac{\mathbb{P}[R_{t_j}(u) = \hat{u}^k]}{m(\overline{B}_{\frac{\alpha}{2}}^\infty \cap R_{t_{\max\{j, j_k\}}}^{-1}(\hat{u}^k))} \int_{\overline{B}_{\frac{\alpha}{2}}^\infty \cap R_{t_{\max\{j, j_k\}}}^{-1}(\hat{u}^k)} |\mathbb{E}_{\xi, b}[\widehat{\nabla} F_i(w + \hat{u}^k, \xi, b) - \widehat{\nabla} F_i(w + u, \xi, b)]| du \\
& \leq \frac{\mathbb{P}[R_{t_j}(u) = \hat{u}^k]}{m(\overline{B}_{\frac{\alpha}{2}}^\infty \cap R_{t_{\max\{j, j_k\}}}^{-1}(\hat{u}^k))} \int_{\overline{B}_{\frac{\alpha}{2}}^\infty \cap R_{t_{\max\{j, j_k\}}}^{-1}(\hat{u}^k)} |\mathbb{E}_{\xi, b}[\widehat{\nabla} F_i(w + \hat{u}^k, \xi, b)]| + |\mathbb{E}_{\xi, b}[\widehat{\nabla} F_i(w + u, \xi, b)]| du \\
& \leq \frac{\mathbb{P}[R_{t_j}(u) = \hat{u}^k]}{m(\overline{B}_{\frac{\alpha}{2}}^\infty \cap R_{t_{\max\{j, j_k\}}}^{-1}(\hat{u}^k))} \int_{\overline{B}_{\frac{\alpha}{2}}^\infty \cap R_{t_{\max\{j, j_k\}}}^{-1}(\hat{u}^k)} \mathbb{E}_{\xi, b}[|\widehat{\nabla} F_i(w + \hat{u}^k, \xi, b)|] + \mathbb{E}_{\xi, b}[|\widehat{\nabla} F_i(w + u, \xi, b)|] du \\
& \leq \frac{\mathbb{P}[R_{t_j}(u) = \hat{u}^k]}{m(\overline{B}_{\frac{\alpha}{2}}^\infty \cap R_{t_{\max\{j, j_k\}}}^{-1}(\hat{u}^k))} \int_{\overline{B}_{\frac{\alpha}{2}}^\infty \cap R_{t_{\max\{j, j_k\}}}^{-1}(\hat{u}^k)} 2\sqrt{c_2 Q} du \\
& \leq 2\sqrt{c_2 Q} \mathbb{P}[R_{t_j}(u) = \hat{u}^k], \quad (33)
\end{aligned}$$

where the second last inequality uses (26) and the fact that almost surely $w + \hat{u}^k$ is not in the set where the bound (12) does not hold using Lemma 24. Given (32) and that there

exists a bounding L^1 function of (27) from (33),

$$\sum_{k=1}^{\infty} 2\sqrt{c_2 Q} \mathbb{P}[R_{t_j}(u) = \hat{u}^k] \leq 2\sqrt{c_2 Q},$$

the dominated convergence theorem can be applied. For almost all $w \in \mathbb{R}^d$, it holds that

$$\begin{aligned} & \lim_{j \rightarrow \infty} \mathbb{E}[\widehat{\nabla} F(w + R_{t_j}(u), \xi, b)] - \mathbb{E}[\widehat{\nabla} F(w + u, \xi, b)] \\ &= \lim_{j \rightarrow \infty} \sum_{k=1}^{\infty} \frac{\mathbb{P}[R_{t_j}(u) = \hat{u}^k]}{m(\overline{B}_{\frac{\alpha}{2}} \cap R_{t_{\max\{j, j_k\}}}^{-1}(\hat{u}^k))} \int_{\overline{B}_{\frac{\alpha}{2}} \cap R_{t_{\max\{j, j_k\}}}^{-1}(\hat{u}^k)} \mathbb{E}_{\xi, b}[\widehat{\nabla} F(w + \hat{u}^k, \xi, b) - \widehat{\nabla} F(w + u, \xi, b)] du \\ &= \sum_{k=1}^{\infty} \lim_{j \rightarrow \infty} \frac{\mathbb{P}[R_{t_j}(u) = \hat{u}^k]}{m(\overline{B}_{\frac{\alpha}{2}} \cap R_{t_{\max\{j, j_k\}}}^{-1}(\hat{u}^k))} \int_{\overline{B}_{\frac{\alpha}{2}} \cap R_{t_{\max\{j, j_k\}}}^{-1}(\hat{u}^k)} \mathbb{E}_{\xi, b}[\widehat{\nabla} F(w + \hat{u}^k, \xi, b) - \widehat{\nabla} F(w + u, \xi, b)] du \\ &= 0. \end{aligned}$$

Applying this result to (24),

$$\begin{aligned} & \lim_{j \rightarrow \infty} \langle \mathbb{E}[\widehat{\nabla} F(w + R_{t_j}(u), \xi, b)], \nabla f_{\alpha}(w) \rangle \\ & \geq \lim_{j \rightarrow \infty} \langle \mathbb{E}[\widehat{\nabla} F(w + R_{t_j}(u), \xi, b)] - \mathbb{E}[\widehat{\nabla} F(w + u, \xi, b)], \nabla f_{\alpha}(w) \rangle + c_1 \|\nabla f_{\alpha}(w)\|_2^2 \\ & \geq c_1 \|\nabla f_{\alpha}(w)\|_2^2. \end{aligned}$$

□

11 Supplementary Material for Section 6

11.1 Choosing the Baseline SGD Model

Training R20C10, momentum = 0.9 and weight decay = 1e-4, following (He et al., 2016, Section 4.2), were tested without rounding these parameter values to avoid biasing these initial experiments. Using FL8N, plotted in Figure 1, it was found that plain SGD worked best: the minimum accuracy of SGD is greater than the maximum accuracy of the momentum variants, and the mean accuracy of SGD is similar to the maximum accuracy when using weight decay. Using FL16N, plotted in Figure 2, SGD+Weight Decay+Momentum has the best accuracy, though in this experiment all methods have relatively similar accuracies. Being significantly better in the lower precision environment, plain SGD was chosen as the baseline SGD algorithm for further low-precision training experiments.

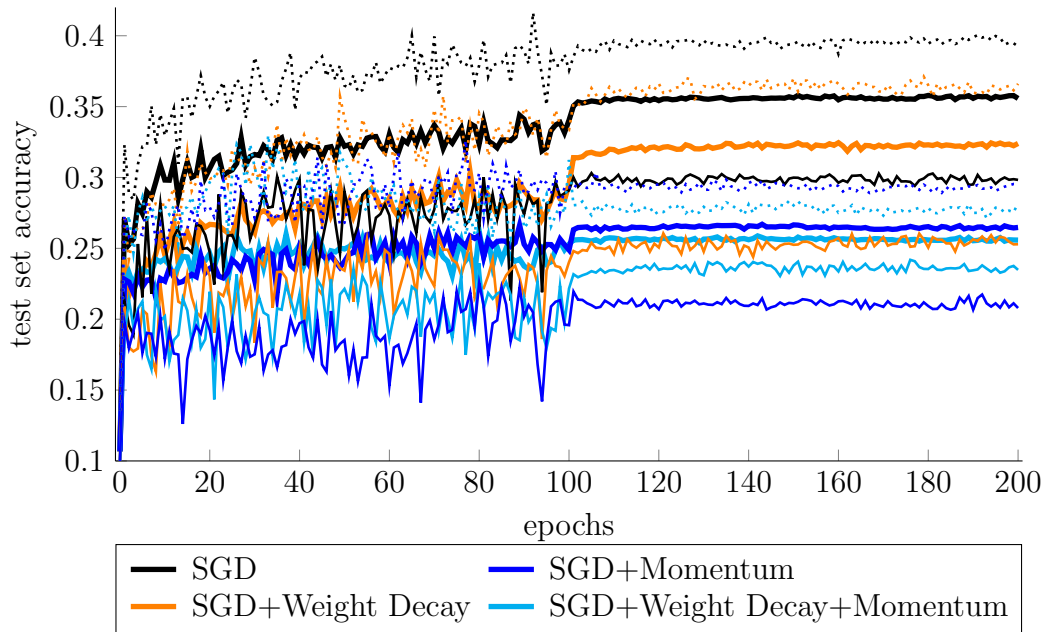


Figure 1: Comparison of popular variants of SGD. The mean (thick solid), minimum (thin solid), and maximum (dotted) test set accuracy over 10 runs of training R20C10 in FL8N is plotted.

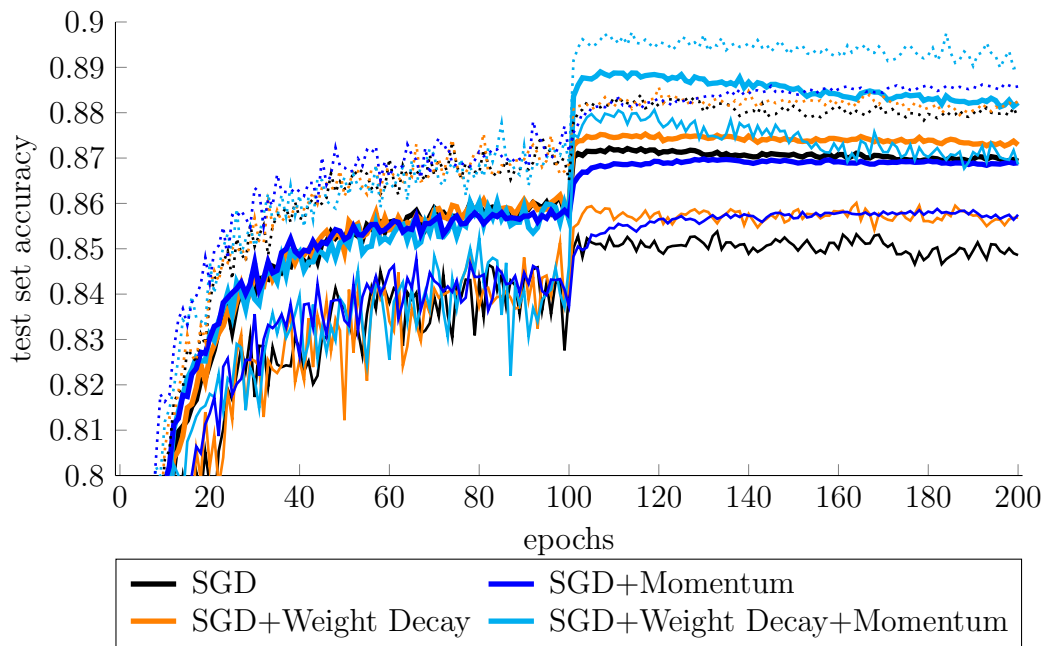


Figure 2: Comparison of popular variants of SGD. The mean (thick solid), minimum (thin solid), and maximum (dotted) test set accuracy over 10 runs of training R20C10 in FL16N is plotted.

11.2 Choosing the Variant of Gradient Normalization

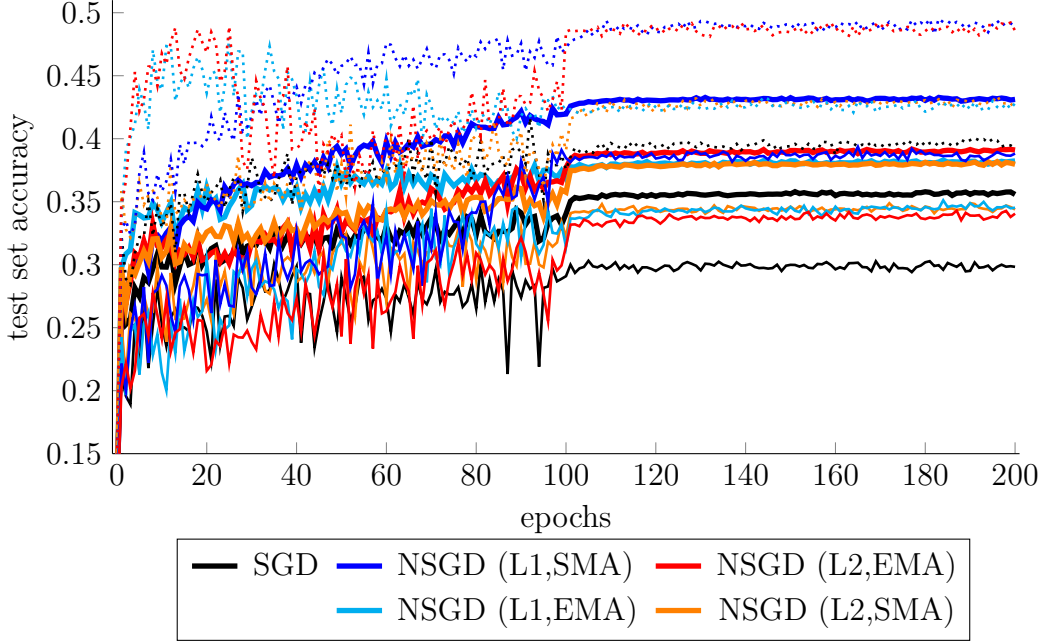


Figure 3: Comparison of different variants of NSGD with SGD. The mean (thick solid), minimum (thin solid), and maximum (dotted) test set accuracy over 10 runs training R20C10 in FL8N is plotted.

11.3 Proof of Proposition 19

Proof. (Proposition 19): If there exists a $\Psi \in \mathbb{F}_{\geq \mu}$ such that $\mathbb{P}(R(\|\widehat{\nabla} \overline{F}(w^k)\|_1) \leq \Psi) = 1$ for all $k \geq 1$, then $\mathbb{P}(\mu \leq m_{ave}^k \leq \Psi) = \mathbb{P}(\mu \leq g_{nrm}^k \leq \Psi) = 1$ for all $k \geq 1$, and

$$\mathbb{P}\left(\frac{\mu}{\Psi} \leq \frac{m_{ave}^{k-1}}{g_{nrm}^{k-1}} \leq \frac{\Psi}{\mu}\right) = 1$$

for all $k > 1$. By assumption then, $\hat{\eta}_k * m_{ave}^{k-1} / g_{nrm}^{k-1} \in [\lambda_N, \Lambda^+]$ almost surely for $k \geq 1$, defining $m_{ave}^0 / g_{nrm}^0 := 1$. For the cases when this holds, the final rounding of Algorithm 1 can be bounded as

$$R(\hat{\eta}_k * m_{ave}^{k-1} / g_{nrm}^{k-1}) = \hat{\eta}_k * m_{ave}^{k-1} / g_{nrm}^{k-1} (1 + \delta)$$

where $|\delta| \leq u$ for rounding to nearest (Higham, 2002, Theorem 2.2) and $|\delta| \leq 2u$ (Connolly et al., 2021, Equation (2.4a)), where $u = \frac{1}{2}\beta^{1-t}$. Setting $\psi_k = m_{ave}^{k-1} / g_{nrm}^{k-1} (1 + \delta)$, it holds that $\mathbb{P}(\Psi^I \leq \psi_k \leq \Psi^S) = 1$ with

$$\Psi^I = \frac{\mu}{\Psi} (1 - 2u) \geq \frac{\mu}{\Psi} (1 - \beta^{-1}) \geq \frac{\mu}{2\Psi},$$

given that $t > 1$ and $\beta > 1$, and $\Psi^S = \frac{\Psi}{\mu} (1 + 2u)$. \square

11.4 Results and Plots of Training in Low-Precision Environments

Table 2: Accuracies, relative accuracies, and scores of all algorithms in the fixed-point rounding to nearest (R=N) and stochastic rounding (R=S) experiments, with the resulting Sum of Accuracies (SoA), Sum of Relative Accuracies (SoR), and Sum of Scores (SoS) methods of ranking. The column Acc indicates whether each row contains the mean or minimum accuracies of each algorithm. Bold and underline indicate the highest and lowest value in each column.

R=N Experiments	Acc	SGD	NSGD	DNSGD	PSGD	PNSGD	PDNSGD
R20C10 FI24/19N	Mean	0.3326	0.3327	<u>0.3309</u>	0.3802	0.3804	0.3814
R20C10 FI24/19N	Min	0.0986	0.0990	0.0996	<u>0.0962</u>	0.0974	0.0981
R32C100 FI26/19N	Mean	<u>0.3690</u>	<u>0.3690</u>	<u>0.3690</u>	0.4274	0.4274	0.4273
R32C100 FI26/19N	Min	0.0100	0.0100	0.0100	0.0100	0.0100	0.0100
SoA		0.8103	0.8107	<u>0.8095</u>	0.9138	0.9152	0.9169
R20C10 FI24/19N	Mean	0.8721	0.8723	<u>0.8676</u>	0.9967	0.9972	1
R20C10 FI24/19N	Min	0.9908	0.9948	1	<u>0.9664</u>	0.9787	0.9858
R32C100 FI26/19N	Mean	<u>0.8634</u>	<u>0.8634</u>	<u>0.8634</u>	1	1	0.9998
R32C100 FI26/19N	Min	<u>0.9993</u>	<u>0.9977</u>	0.9987	1	1	1
SoR		<u>3.7256</u>	3.7281	3.7298	3.9631	3.9760	3.9856
R20C10 FI24/19N	Mean	<u>-3</u>	<u>-3</u>	<u>-3</u>	3	3	3
R20C10 FI24/19N	Min	0	0	0	0	0	0
R32C100 FI26/19N	Mean	<u>-3</u>	<u>-3</u>	<u>-3</u>	3	3	3
R32C100 FI26/19N	Min	0	0	0	0	0	0
SoS		<u>-6</u>	<u>-6</u>	<u>-6</u>	6	6	6

R=S Experiments	Acc	SGD	NSGD	DNSGD	PSGD	PNSGD	PDNSGD
R20C10 FI20/15S	Mean	0.8640	0.8601	0.8588	0.8608	0.8641	<u>0.8564</u>
R20C10 FI20/15S	Min	0.8456	0.8507	0.8475	0.8484	0.8566	<u>0.8326</u>
R32C100 FI24/17S	Mean	<u>0.5902</u>	0.5982	0.5973	0.5953	0.6015	0.6013
R32C100 FI24/17S	Min	<u>0.5749</u>	0.5754	0.5850	0.5794	0.5872	0.5873
SoA		<u>2.8745</u>	2.8845	2.8886	2.8840	2.9094	2.8777
R20C10 FI20/15S	Mean	0.9998	0.9954	0.9938	0.9962	1	<u>0.9911</u>
R20C10 FI20/15S	Min	0.9871	0.9931	0.9893	0.9905	1	<u>0.9720</u>
R32C100 FI24/17S	Mean	<u>0.9812</u>	0.9945	0.9931	0.9898	1	0.9997
R32C100 FI24/17S	Min	<u>0.9788</u>	0.9797	0.9961	0.9866	0.9998	1
SoR		<u>3.9469</u>	3.9628	3.9722	3.9629	3.9998	3.9629
R20C10 FI20/15S	Mean	4	<u>-2</u>	<u>-2</u>	<u>-2</u>	4	-2
R20C10 FI20/15S	Min	-1	3	-1	-1	5	<u>-5</u>
R32C100 FI24/17S	Mean	<u>-5</u>	-1	-1	-1	4	4
R32C100 FI24/17S	Min	<u>-3</u>	<u>-3</u>	3	<u>-3</u>	3	3
SoS		-5	-3	-1	<u>-7</u>	16	0

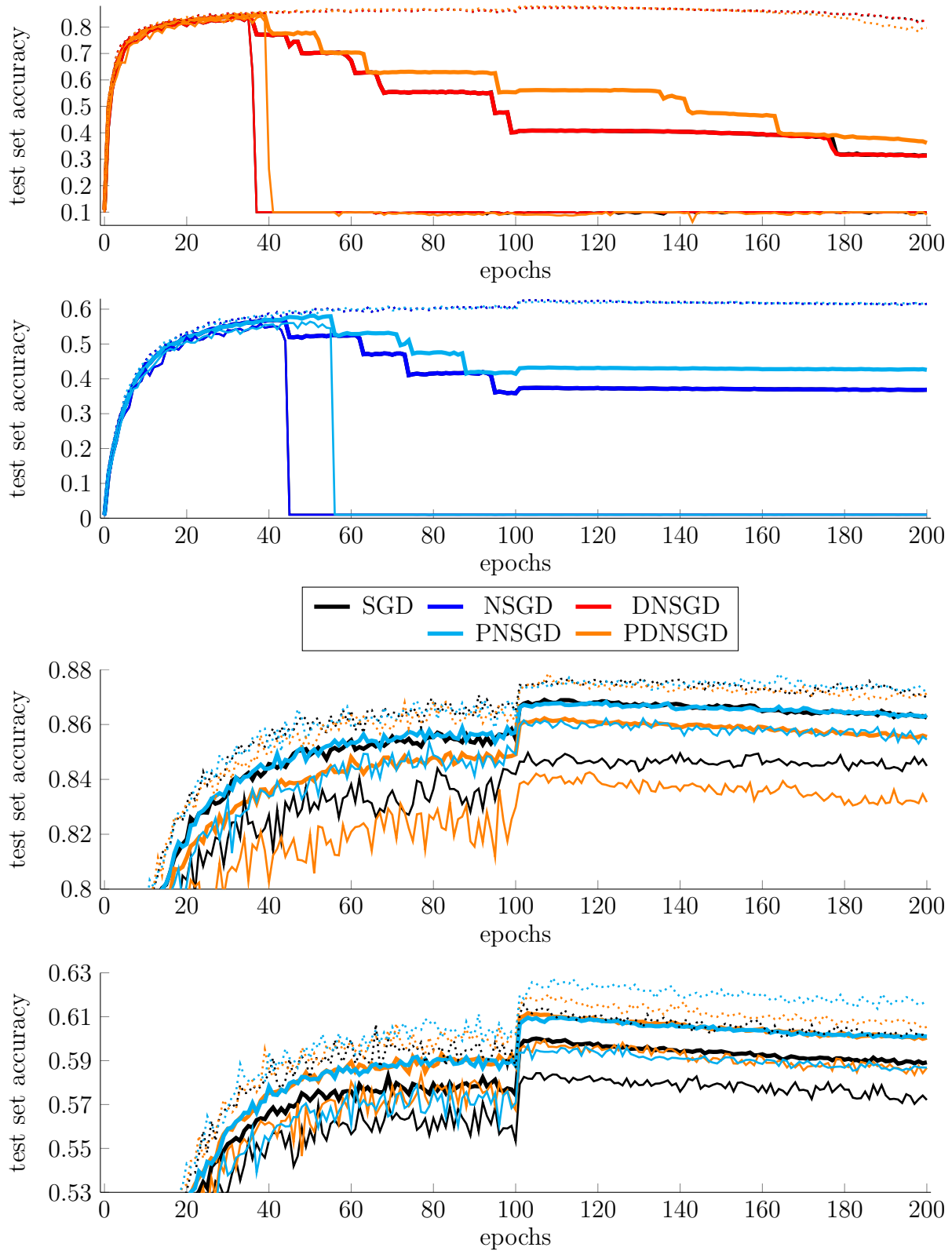


Figure 4: Plots of SGD and the best and worst performing algorithms. The mean (thick solid), minimum (thin solid), and maximum (dotted) test set accuracy from training, from top to bottom, R20C10 in FI24/19N, R32C100 in FI26/19N, R20C10 in FI20/15S, and R32C100 in FI24/17S over 10 runs is plotted.

Table 3: Accuracies, relative accuracies, and scores of all algorithms in the floating-point rounding to nearest experiments, with the resulting Sum of Accuracies (SoA), Sum of Relative Accuracies (SoR), and Sum of Scores (SoS) methods of ranking. The column Acc indicates whether each row contains the mean or minimum accuracies of each algorithm. Bold and underline indicate the highest and lowest value in each column.

R=N Experiments	Acc	SGD	NSGD	DNSGD	PSGD	PNSGD	PDNSGD
R20C10 FL8N	Mean	0.3565	0.4315	0.3683	<u>0.3226</u>	0.3890	0.3673
R20C10 FL8N	Min	0.2984	0.3868	0.3180	<u>0.2798</u>	0.2950	0.3038
R20C10 FL9N	Mean	0.7804	0.7730	0.7744	0.7730	0.7706	<u>0.7655</u>
R20C10 FL9N	Min	0.7359	0.7620	0.7592	0.7344	0.7587	<u>0.7018</u>
R32C100 FL9N	Mean	0.1974	0.2052	0.2043	0.1840	<u>0.1837</u>	0.1854
R32C100 FL9N	Min	0.1590	0.1750	0.1755	0.1572	<u>0.1515</u>	0.1674
R32C100 FL10N	Mean	0.4369	0.4405	<u>0.4344</u>	0.4347	0.4372	0.4356
R32C100 FL10N	Min	0.4250	0.4214	<u>0.4213</u>	0.4229	0.4258	0.4263
SoA		3.3896	3.5955	3.4552	<u>3.3086</u>	3.4115	3.3531
R20C10 FL8N	Mean	0.8263	1	0.8537	<u>0.7477</u>	0.9015	0.8514
R20C10 FL8N	Min	0.7714	1	0.8220	<u>0.7233</u>	0.7626	0.7854
R20C10 FL9N	Mean	1	0.9905	0.9923	0.9905	0.9875	<u>0.9809</u>
R20C10 FL9N	Min	0.9657	1	0.9962	0.9637	0.9956	<u>0.9209</u>
R32C100 FL9N	Mean	0.9618	1	0.9955	0.8969	<u>0.8954</u>	0.9034
R32C100 FL9N	Min	0.9063	0.9975	1	0.8959	<u>0.8636</u>	0.9539
R32C100 FL10N	Mean	0.9919	1	<u>0.9861</u>	0.9868	0.9926	0.9889
R32C100 FL10N	Min	0.9970	0.9886	<u>0.9882</u>	0.9922	0.9988	1
SoR		7.4205	7.9766	7.6340	<u>7.1970</u>	7.3975	7.3849
R20C10 FL8N	Mean	-3	5	0	<u>-5</u>	3	0
R20C10 FL8N	Min	-2	5	3	<u>-5</u>	-2	1
R20C10 FL9N	Mean	5	0	0	0	0	<u>-5</u>
R20C10 FL9N	Min	-2	3	3	-2	3	<u>-5</u>
R32C100 FL9N	Mean	1	4	4	<u>-3</u>	<u>-3</u>	<u>-3</u>
R32C100 FL9N	Min	-2	4	4	-2	<u>-5</u>	1
R32C100 FL10N	Mean	<u>-1</u>	5	<u>-1</u>	<u>-1</u>	<u>-1</u>	<u>-1</u>
R32C100 FL10N	Min	3	<u>-3</u>	<u>-3</u>	<u>-3</u>	3	3
SoS		-1	23	10	<u>-21</u>	-2	-9

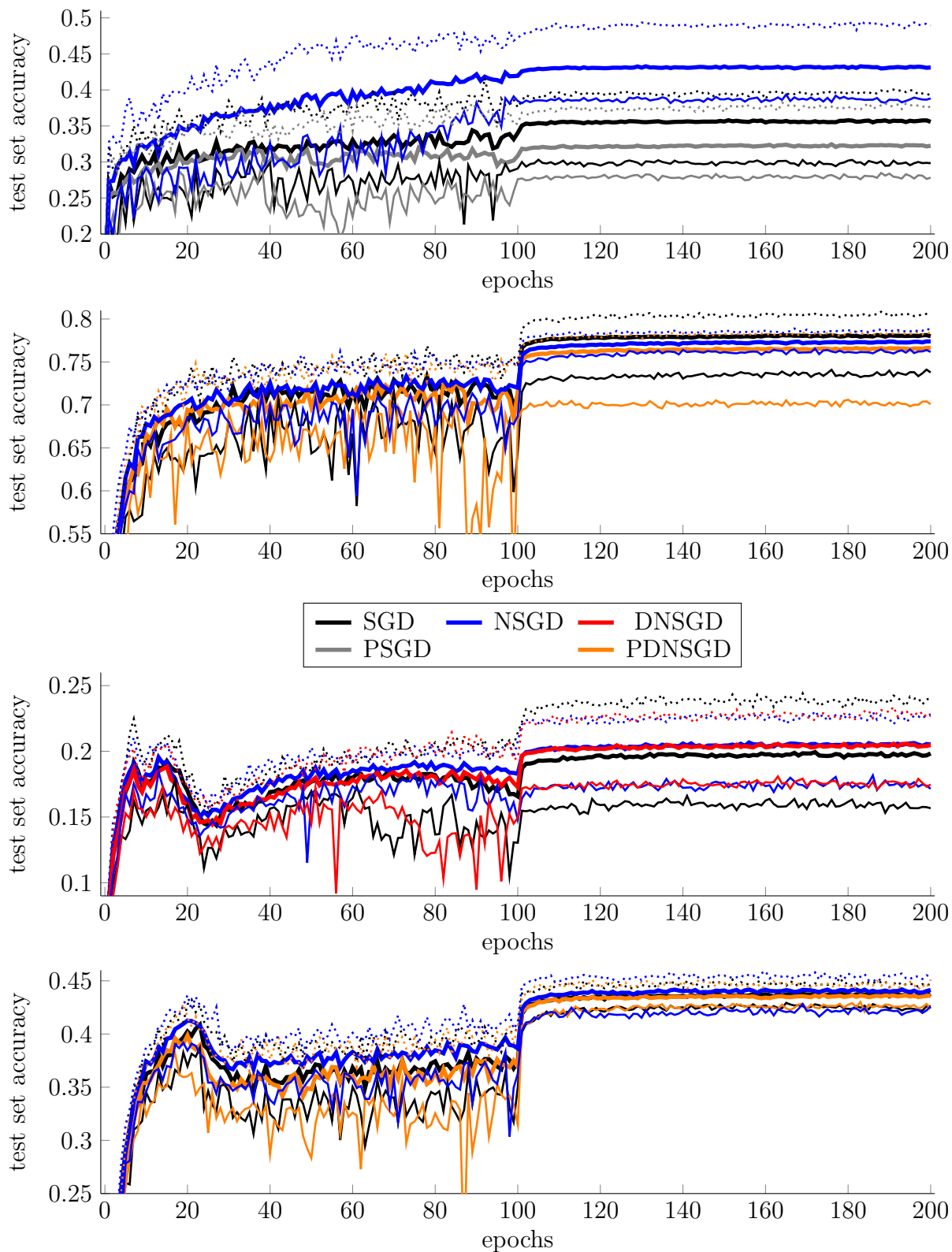


Figure 5: Plots of SGD and the best (and worst) performing algorithms. The mean (thick solid), minimum (thin solid), and maximum (dotted) test set accuracy from training, from top to bottom, R20C10 in FL8N, R20C10 in FL9N, R32C100 in FL9N, and R32C100 in FL10N over 10 runs is plotted.

Table 4: Accuracies, relative accuracies, and scores of all algorithms in the floating-point stochastic rounding experiments, with the resulting Sum of Accuracies (SoA), Sum of Relative Accuracies (SoR), and Sum of Scores (SoS) methods of ranking. The column Acc indicates whether each row contains the mean or minimum accuracies of each algorithm. Bold and underline indicate the highest and lowest value in each column.

R=S Experiments	Acc	SGD	NSGD	DNSGD	PSGD	PNSGD	PDNSGD
R20C10 FL8S	Mean	0.4559	0.4644	0.4873	0.4709	0.4844	<u>0.4404</u>
R20C10 FL8S	Min	0.3912	0.4271	0.4316	0.4285	0.4069	<u>0.3907</u>
R20C10 FL8S WD	Mean	0.5130	<u>0.5094</u>	0.5159	0.5144	0.5211	0.5292
R20C10 FL8S WD	Min	0.4764	<u>0.4242</u>	0.4735	0.4590	0.4828	0.4814
R32C100 FL9S	Mean	0.3776	0.3746	0.3695	0.3716	0.3826	<u>0.3679</u>
R32C100 FL9S	Min	0.3504	<u>0.3489</u>	0.3512	0.3558	0.3682	0.3518
R32C100 FL9S WD	Mean	0.4072	<u>0.3994</u>	0.4023	0.4121	0.4100	0.4084
R32C100 FL9S WD	Min	0.3864	0.3794	<u>0.3789</u>	0.3900	0.3940	0.3906
SoA		<u>2.8745</u>	2.8845	2.8886	2.8840	2.9094	2.8777
R20C10 FL8S	Mean	0.9356	0.9531	1	0.9663	0.9940	<u>0.9038</u>
R20C10 FL8S	Min	0.9065	0.9895	1	0.9928	0.9427	<u>0.9051</u>
R20C10 FL8S WD	Mean	0.9694	<u>0.9627</u>	0.9750	0.9722	0.9848	1
R20C10 FL8S WD	Min	0.9867	<u>0.8787</u>	0.9807	0.9507	1	0.9972
R32C100 FL9S	Mean	0.9870	0.9791	0.9657	0.9712	1	<u>0.9616</u>
R32C100 FL9S	Min	0.9518	<u>0.9477</u>	0.9537	0.9663	1	0.9555
R32C100 FL9S WD	Mean	0.9880	<u>0.9692</u>	0.9762	1	0.9949	0.9910
R32C100 FL9S WD	Min	0.9807	0.9629	<u>0.9617</u>	0.98980	1	0.99120
SoR		7.7057	<u>7.6428</u>	7.8131	7.8092	7.9163	7.7054
R20C10 FL8S	Mean	-3	-1	4	1	4	<u>-5</u>
R20C10 FL8S	Min	<u>-4</u>	3	3	3	-1	<u>-4</u>
R20C10 FL8S WD	Mean	-1	<u>-5</u>	-1	-1	3	5
R20C10 FL8S WD	Min	0	<u>-5</u>	0	-3	4	4
R32C100 FL9S	Mean	2	2	<u>-3</u>	<u>-3</u>	5	<u>-3</u>
R32C100 FL9S	Min	<u>-2</u>	<u>-2</u>	<u>-2</u>	3	5	<u>-2</u>
R32C100 FL9S WD	Mean	2	<u>-4</u>	<u>-4</u>	2	2	2
R32C100 FL9S WD	Min	-1	<u>-4</u>	<u>-4</u>	3	3	3
SoS		-7	<u>-16</u>	-7	5	25	0

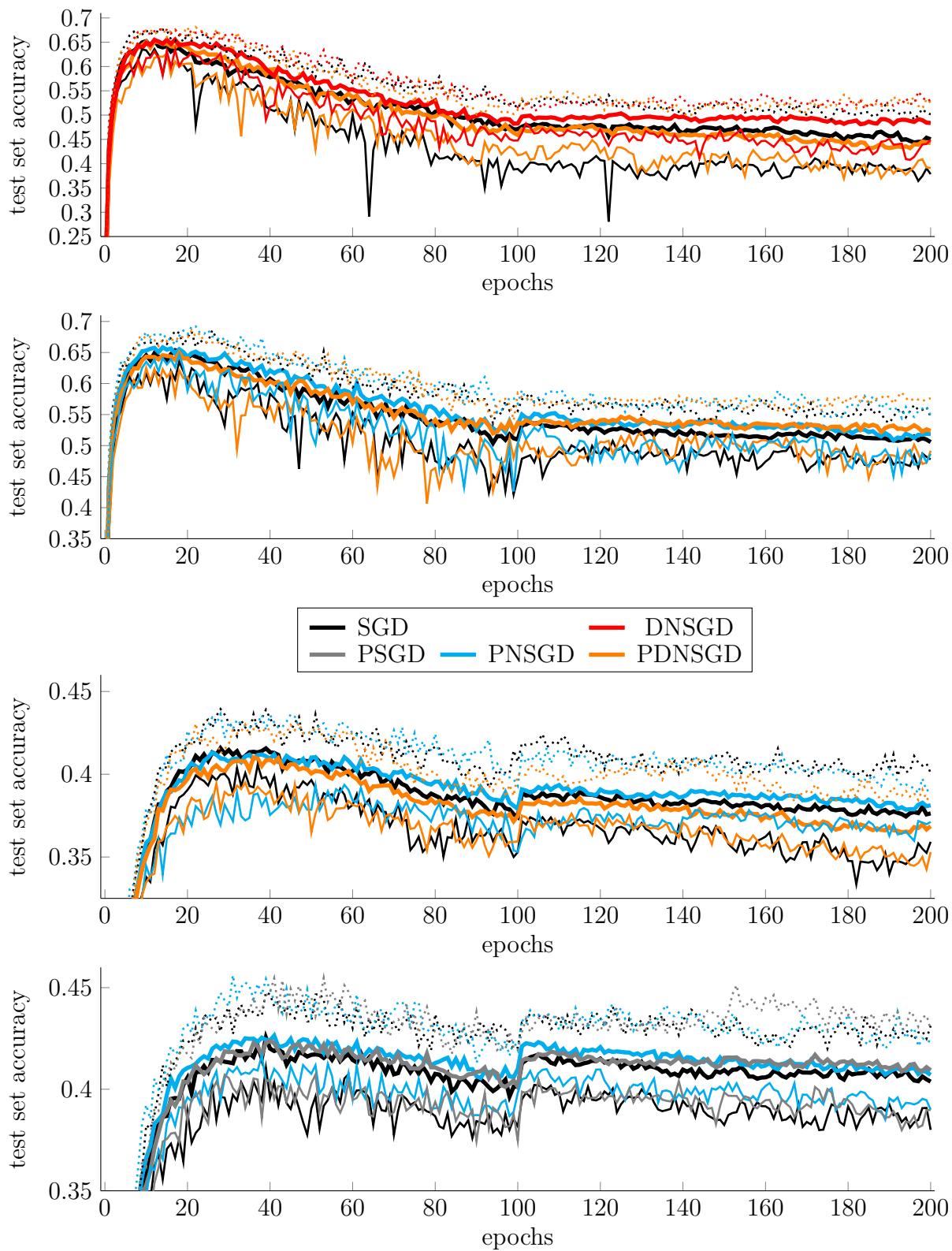


Figure 6: Plots of SGD and the best (and worst) performing algorithms. The mean (thick solid), minimum (thin solid), and maximum (dotted) test set accuracy from training, from top to bottom, R20C10 in FL8S, R20C10 in FL8S with weight decay (WD), R32C100 in FL9S, and R32C100 in FL9S with WD over 10 runs is plotted.